Philosophical Magazine
Vol. 00, No. 00, 00 Month 2010, 1–36

RESEARCH ARTICLE

An incremental-secant mean-field homogenisation method with second statistical moments for elasto-plastic composite materials

L. Wu[a*], I. Doghri[b] and L. Noels[a]

[a] *University of Liège Computational & Multiscale Mechanics of Materials, Chemin des Chevreuils 1, B-4000 Liège, Belgium*;
[b] *Université catholique de Louvain, Institute of Mechanics, Materials and Civil Engineering, Bâtiment Euler, 1348 Louvain-la-Neuve, Belgium*

(*v4.5 released May 2010*)

In this paper, the incremental-secant mean-field homogenisation (MFH) scheme recently developed by the authors is extended to account for second statistical moments.

The incremental-secant MFH method possesses several advantages compared to other MFH methods. Indeed the method can handle non-proportional and non-monotonic loadings, while the instantaneous stiffness operators used in the Eshelby tensor are naturally isotropic, avoiding the isotropisation approximation required by the affine and incremental-tangent methods. Moreover, the incremental-secant MFH formalism was shown to be able to account for material softening when extended to include a non-local damage model in the matrix phase, thus enabling an accurate simulation of the onset and evolution of damage across the scales.

In this work, by accounting for a second statistical moment estimation of the current yield stress in the composite phases, the plastic flow computation allows capturing with a better accuracy the plastic yield in the composite material phases, which in turn improves the accuracy of the predictions, mainly in the case of short fibre composite materials. The incremental-secant mean-field-homogenisation (MFH) can thus be used to model a wide variety of composite material systems with a good accuracy.

Keywords: Multi-scale; Mean-Field Homogenisation; Composites; Second Statistical Moments;

1. Introduction

With the emergence of new engineered materials such as composite materials, multi-scale simulations are gaining popularity as they provide an efficient way to predict the macroscopic response of a structure made of heterogeneous materials from the micro-scale information, such as the micro-structure and the micro-constituents behaviour. A popular multi-scale approach relies on the prediction of the macroscopic stress-strain relation of the heterogeneous material under the form of a homogenised constitutive law to be used in a macro-scale problem. This homogeneous constitutive law can be obtained by using analytical or numerical methods, or a combination of both, see [1, 2] for an overview.

The first statistical moment mean-field homogenisation (MFH) method seeks the macroscopic stress–strain relation by considering the average values, of the different fields, in each phase of a heterogeneous material. Most of MFH methods are based on the extension from the single inclusion Eshelby [3] solution to the

*Corresponding author. Email: l.wu@ulg.ac.be

ISSN: 1478-6435 print/ISSN 1478-6443 online

DOI: 10.1080/14786435.20xx.xxxxxx
http://www.informaworld.com

interaction of multiple inclusions. This extension requires assumptions on these interactions, the most common ones being the Mori–Tanaka scheme [4, 5] and the self–consistent model [6, 7]. As these models assume a linear relation between the average stress and strain of the constituents, the extension to non-linear material behaviours is based on the definition of a linear comparison composite (LCC) [8–13], which is a virtual composite whose constituents linear behaviours match the linearised behaviour of the real constituents for a given strain state. Thus the MFH methods for linear responses can be applied on this LCC, allowing to model non-linear composite material responses.

The LCC can be defined under several forms. In the incremental–tangent formulation [14–18], linearised relations between the stress and strain increments of the different constituents are considered around their current strain states. The affine method considers a linearised behaviour on the total strain field, in which case the stress increment is computed from a polarisation stress [13, 19–24]. Both the incremental-tangent method [16, 18] and the affine method [25] can exhibit over-stiff results unless some isotropic projections of the tangent operator is considered in the homogenisation process. In the secant method [26], the linearised law is pseudo-elastic in terms of total stress and strain, which limits the method to monotonic and proportional loading paths.

In order to avoid the isotropisation step while keeping the accuracy of the method in case of non-proportional loading, an incremental-secant formulation, in which a secant stiffness links, in each phase, the current stress/strain state to a residual state, has recently been proposed by the authors [27]. The residual state is obtained upon a virtual elastic unloading of the composite material. Besides these two advantages, *i.e.* the method directly provides isotropic instantaneous stiffness operators, avoiding the isotropisation step, and the method remains accurate in case of non-monotonic and non-proportional loadings, the method is of particular interest when considering material behaviour with strain softening [28, 29]. Indeed, because the secant formulation is applied from a virtually unloaded state, one phase of the composite material can be elastically unloaded during the softening of the other phase, contrarily to what happens with an incremental-tangent method [29]. In this last case, a Lemaitre-Chaboche damage model [30, 31] formulated in non-local way [32–35] is adopted. The non-local formulation of the damage evolution is required in order to avoid the loss of the solution uniqueness caused by the material softening.

Despite the accurate predictions obtained with the incremental-secant method in most cases, even for highly non-linear elasto-plastic behaviours, for short fibre composite materials the method is still over-predicting the composite response. Indeed as, at the time being, the developed formulation [27] uses only the average stress tensor to predict the plastic flow in the different phases, the plastic yield is not accurately captured. This is typical of mean-field homogenisation schemes using only the first statistical moment values, *i.e.* only the average values of the different fields. In this paper in order to improve the accuracy of the incremental-secant method, it is intended to extend it to account for the second statistical moment value of the von Mises stress during the homogenisation process.

Second statistical moments were already considered in the MFH process to improve the prediction in the elasto-plastic case [36, 37], in particular for the secant formulations [38–40] and for the incremental–tangent formulation [41]. The variational forms pioneered by [11] is a second-order secant formulation, also called modified-secant MFH, as demonstrated in [38]. Finally, the incremental variational formulations recently proposed for visco-elastic and elasto-(visco-)plastic composite materials by [42–47] also account for the second statistical moment.

This paper is organised as follows. In Section 2, the main ideas and equations of the MFH are briefly recalled. In particular the linear-comparison-composite (LCC) used for non-linear material models is defined. The incremental-secant formulation of an elasto-plastic material is developed in Section 3, first as a local field and then in an averaged way using first and second statistical moment estimations. Based on this averaged incremental-secant formulation of a material law, the incremental-secant MFH of non-linear composite materials is developed and detailed in Section 4. Finally the accuracy of the developed method is investigated in Section 5, where it is shown that the advantages of the incremental-secant MFH formulation are kept when considering the second statistical moment estimations, while the predictions are more accurate in the case of short-fibre composite materials. The advantages of the method and its limitations in the case of perfectly-plastic inclusions composite materials are discussed in Section 6. The perspectives of the developed incremental-secant MFH with second statistical moment estimations, in particular in the case of non-local damage-enhanced elasto-plastic material laws, are also discussed in this section, before drawing the general conclusions.

2. Generalities on the mean-field homogenisation for two-phase composites

In a multiscale approach, at each macro-point $\boldsymbol{X}$ of the structure, the resolution of a micro-scale boundary value problem (BVP) relates the macro-stress tensor $\bar{\boldsymbol{\sigma}}$ to the macro-strain tensor $\bar{\boldsymbol{\varepsilon}}$. At the micro-level, the macro-point is viewed as the centre of a RVE of domain ω.

Because of the energy equivalence at the two scales, the Hill-Mandell condition implies the relation between the macro-strains $\bar{\boldsymbol{\varepsilon}}$ and stresses $\bar{\boldsymbol{\sigma}}$ to be equivalent to the relation between the volume average of the strain tensor $\langle\boldsymbol{\varepsilon}\rangle_\omega$ and stress tensor $\langle\boldsymbol{\sigma}\rangle_\omega$ over the RVE. For a two-phase isothermal composite material with the respective volume fractions $v_0 + v_\mathrm{I} = 1$ (subscript 0 refers to the matrix and I to the inclusions), the average quantities are expressed in terms of the phase averages as

$$\bar{\boldsymbol{\varepsilon}} = v_0\langle\boldsymbol{\varepsilon}\rangle_{\omega_0} + v_\mathrm{I}\langle\boldsymbol{\varepsilon}\rangle_{\omega_\mathrm{I}} \quad \text{and} \quad \bar{\boldsymbol{\sigma}} = v_0\langle\boldsymbol{\sigma}\rangle_{\omega_0} + v_\mathrm{I}\langle\boldsymbol{\sigma}\rangle_{\omega_\mathrm{I}}\,. \tag{1}$$

In the following developments, the notations $\bar{\bullet}_i$ hold for $\langle\bullet\rangle_{\omega_i}$.

By defining a linear comparison composite (LCC) representing the linearised behaviour of the composite material phases through their virtual elastic operators, $\hat{\mathbb{C}}_0^{\mathrm{LCC}}$ for the matrix phase and $\hat{\mathbb{C}}_\mathrm{I}^{\mathrm{LCC}}$ for the inclusions phase, the relation between the average strain increments reads

$$\Delta\bar{\boldsymbol{\varepsilon}}_\mathrm{I} = \mathbb{B}^\epsilon(\mathrm{I}, \hat{\mathbb{C}}_0^{\mathrm{LCC}}, \hat{\mathbb{C}}_\mathrm{I}^{\mathrm{LCC}}) : \Delta\bar{\boldsymbol{\varepsilon}}_0\,. \tag{2}$$

In this paper, the Mori-Tanaka (M-T) expression of the strain concentration tensor $\mathbb{B}^\epsilon$ is used, *i.e.*

$$\mathbb{B}^\epsilon = \{\mathbb{I} + \mathbb{S} : [(\hat{\mathbb{C}}_0^{\mathrm{LCC}})^{-1} : \hat{\mathbb{C}}_\mathrm{I}^{\mathrm{LCC}} - \mathbb{I}]\}^{-1}\,, \tag{3}$$

where the Eshelby tensor [3] $\mathbb{S}(\mathrm{I}, \hat{\mathbb{C}}_0^{\mathrm{LCC}})$ depends on the geometry of the inclusion (I) and on the matrix phase virtual pseudo-elastic operator $\hat{\mathbb{C}}_0^{\mathrm{LCC}}$.

The expressionss of the tensors $\hat{\mathbb{C}}_0^{\mathrm{LCC}}$ and $\hat{\mathbb{C}}_\mathrm{I}^{\mathrm{LCC}}$ result from the assumptions behind the MFH formulation. In linear elasticity, they reduce to the elastic material fourth order tensors $\mathbb{C}_0^{\mathrm{el}}$ and $\mathbb{C}_\mathrm{I}^{\mathrm{el}}$. For non-linear behaviours, they are constructed

to be uniform, hence the $\hat{\bullet}$ notation. With the incremental-tangent MFH method, they correspond to the "consistent" average tangential operators $\hat{\mathbb{C}}_0^{\text{alg}}$ and $\hat{\mathbb{C}}_{\text{I}}^{\text{alg}}$, and with the incremental-secant formalism [27] considered in this work, they correspond to the secant operators $\hat{\mathbb{C}}_0^{\text{S}}$ and $\hat{\mathbb{C}}_{\text{I}}^{\text{S}}$. In particular, the secant operator of the matrix phase is naturally isotropic for J2-elasto-plastic materials, which prevents the isotropisation step required with the incremental-tangent method [18].

In the context of elasto-plastic materials, besides the first statistical moment values, $\langle\bullet\rangle_{\omega_i} = \bar{\bullet}_i$ of the stress and strain (increment) fields, the second statistical moment of the stress and strain increment fields $\langle\bullet\otimes\bullet\rangle_{\omega_i}$ are also of interest to compute the plastic flow. In particular, one can compute in the phase i the second statistical moment of the equivalent strain increment

$$\Delta\hat{\bar{\varepsilon}}_i^{\text{eq}} = \sqrt{\frac{2}{3}\mathbb{I}^{\text{dev}} :: \langle\Delta\boldsymbol{\varepsilon}\otimes\Delta\boldsymbol{\varepsilon}\rangle_{\omega_i}}\,, \tag{4}$$

and of the equivalent stress increment

$$\Delta\hat{\bar{\sigma}}_i^{\text{eq}} = \sqrt{\frac{3}{2}\mathbb{I}^{\text{dev}} :: \langle\Delta\boldsymbol{\sigma}\otimes\Delta\boldsymbol{\sigma}\rangle_{\omega_i}}\,. \tag{5}$$

where $\mathbb{I}^{\text{dev}}$ is the deviatoric fourth order tensor.

3. Incremental-secant formulation of elasto-plastic materials with second statistical moment estimations

In this section the secant formulation of J2-elasto-plastic behaviours is presented. First generalities on J2-plasticity are recalled and then the local and second statistical moment enhanced incremental-secant formulations are detailed.

3.1. *J2-plasticity*

The elasto-plastic material formulation under the J2-elasto-plasticity assumption is characterised by the von Mises yield criterion, which reads

$$f\left(\boldsymbol{\sigma}\left(\boldsymbol{x}\right), p\left(\boldsymbol{x}\right)\right) = \sigma^{\text{eq}}\left(\boldsymbol{x}\right) - R\left(p\left(\boldsymbol{x}\right)\right) - \sigma_Y \leq 0 \quad \forall\boldsymbol{x}\in\omega_i\,, \tag{6}$$

where f is the yield surface,

$$\sigma^{\text{eq}} = \left(\boldsymbol{\sigma}\right)^{\text{eq}} = \sqrt{\frac{3}{2}\boldsymbol{\sigma} : \mathbb{I}^{\text{dev}} : \boldsymbol{\sigma}}\,, \tag{7}$$

is the equivalent von Mises stress, σ_Y is the initial yield stress, and $R(p) \geqslant 0$ is the isotropic hardening stress in terms of p the accumulated plastic strain. During the plastic flow, *i.e.* $f = 0$, $\Delta p > 0$, the plastic strain rate tensor follows the plastic flow direction

$$\dot{\boldsymbol{\varepsilon}}^{\text{p}}\left(\boldsymbol{x}\right) = \dot{p}\left(\boldsymbol{x}\right)\frac{\partial f\left(\boldsymbol{x}\right)}{\partial\boldsymbol{\sigma}} = \dot{p}\left(\boldsymbol{x}\right)\boldsymbol{N}\left(\boldsymbol{x}\right) \quad \forall\boldsymbol{x}\in\omega_i\,, \tag{8}$$

where $\boldsymbol{N}$ is the normal to the yield surface in the stress space. The stress tensor follows from

$$\boldsymbol{\sigma}(\boldsymbol{x}) = \mathbb{C}_i^{\mathrm{el}} : \boldsymbol{\varepsilon}^{\mathrm{el}}(\boldsymbol{x}) = \mathbb{C}_i^{\mathrm{el}} : (\boldsymbol{\varepsilon}(\boldsymbol{x}) - \boldsymbol{\varepsilon}^{\mathrm{p}}(\boldsymbol{x})) \quad \forall \boldsymbol{x} \in \omega_i \,, \tag{9}$$

with the material elastic tensor in phase i

$$\mathbb{C}_i^{\mathrm{el}} = 3\kappa_i^{\mathrm{el}} \mathbb{I}^{\mathrm{vol}} + 2\mu_i^{\mathrm{el}} \mathbb{I}^{\mathrm{dev}} \,, \tag{10}$$

expressed in terms of the elastic bulk and shear moduli.

3.2. *Incremental-secant approach*

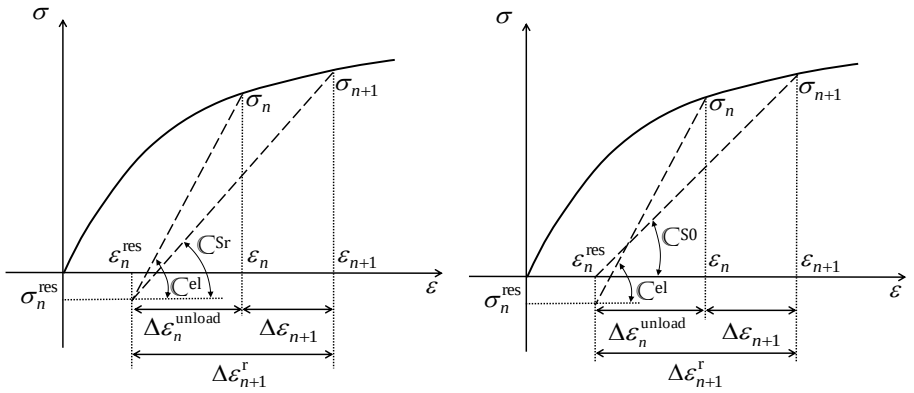

(a) Residual-incremental-secant approach (b) Zero-incremental-secant approach

Figure 1. Schematics of the incremental-secant formulations from [27]. (a) The residual-incremental-secant operator is defined from the residual strain and stress. (b) The zero-incremental-secant operator is defined from the residual strain at a zero-stress state.

The elasto-plastic material model can be presented under an incremental-secant formulation. Considering a time interval $[t_n,\ t_{n+1}]$, with the total strain tensor $\boldsymbol{\varepsilon}_n$ at time t_n known and the strain increment $\Delta\boldsymbol{\varepsilon}_{n+1}$ resulting from the incremental resolution scheme supposed given, the strain tensor $\boldsymbol{\varepsilon}_{n+1}$ at time t_{n+1} follows from

$$\boldsymbol{\varepsilon}_{n+1}(\boldsymbol{x}) = \boldsymbol{\varepsilon}_n(\boldsymbol{x}) + \Delta\boldsymbol{\varepsilon}_{n+1}(\boldsymbol{x}) \quad \forall \boldsymbol{x} \in \omega_i \,. \tag{11}$$

At time t_n, a virtual elastic unloading step from the stress state $\boldsymbol{\sigma}_n$ is applied, which corresponds to a residual strain tensor $\boldsymbol{\varepsilon}_n^{\mathrm{res}}$, see Fig. 1(a). In the incremental-secant framework, a LCC is defined so that the composite phases are subjected to a strain increment $\Delta\boldsymbol{\varepsilon}_{n+1}^{\mathrm{r}}$, satisfying

$$\boldsymbol{\varepsilon}_{n+1}(\boldsymbol{x}) = \boldsymbol{\varepsilon}_n^{\mathrm{res}}(\boldsymbol{x}) + \Delta\boldsymbol{\varepsilon}_{n+1}^{\mathrm{r}}(\boldsymbol{x}) \quad \forall \boldsymbol{x} \in \omega_i \,. \tag{12}$$

To compute the stress tensor at time t_{n+1}, the two methods illustrated in Fig. 1 can be applied. The residual-incremental-secant method computes the effective stress tensor from the residual effective stress obtained after the virtual elastic unloading, while the zero-incremental-secant method computes the effective stress tensor from a zero-stress state (but not from a zero-strain-state). Indeed, with a view to the MFH of composite materials, as lengthy discussed in [27], to accurately capture the elasto-plastic behaviour of the matrix phase when the matrix residual stress is located on the other side of the origin than the current stress state, the

secant approach has to be applied in the matrix phase from a fictitious unloaded state corresponding to a residual strain for a stress state sets to zero. In other words in the case of inclusions remaining elastic, or exhibiting an elasto-plastic behaviour with a derivative of the hardening law higher than the one of the elasto-plastic matrix material, the residual stress (but not strain) in the matrix phase was canceled.

3.2.1. Residual-incremental-secant approach

At first, a virtual elastic unloading is applied from the solution at time t_n, see Fig. 1(a), leading to the residual stress

$$\boldsymbol{\sigma}_n^{\mathrm{res}}(\boldsymbol{x}) = \boldsymbol{\sigma}_n(\boldsymbol{x}) - \mathbb{C}_i^{\mathrm{el}} : \Delta\boldsymbol{\varepsilon}_n^{\mathrm{unload}}(\boldsymbol{x}) = \boldsymbol{\sigma}_n(\boldsymbol{x}) - \Delta\boldsymbol{\sigma}_n^{\mathrm{unload}}(\boldsymbol{x}) \quad \forall \boldsymbol{x} \in \omega_i \,. \tag{13}$$

Practically the unloading strain increment $\Delta\boldsymbol{\varepsilon}_n^{\mathrm{unload}}$ can be chosen so that the homogenised residual stress of a composite material vanishes, as it will be discussed in the MFH section.

Following the method pictured on Fig. 1(a), the stress tensor $\boldsymbol{\sigma}_{n+1}$ at time t_{n+1} can also be expressed as

$$\boldsymbol{\sigma}_{n+1}(\boldsymbol{x}) = \boldsymbol{\sigma}_n^{\mathrm{res}}(\boldsymbol{x}) + \Delta\boldsymbol{\sigma}_{n+1}^{\mathrm{r}}(\boldsymbol{x}) \quad \forall \boldsymbol{x} \in \omega_i \,, \tag{14}$$

with

$$\Delta\boldsymbol{\sigma}_{n+1}^{\mathrm{r}}(\boldsymbol{x}) = \mathbb{C}^{\mathrm{Sr}}(\boldsymbol{x}) : \Delta\boldsymbol{\varepsilon}_{n+1}^{\mathrm{r}}(\boldsymbol{x}) \quad \forall \boldsymbol{x} \in \omega_i \,, \tag{15}$$

where $\mathbb{C}^{\mathrm{Sr}}$ is the residual-incremental-secant operator of the linear comparison material. The Cauchy stress tensor at time t_{n+1} is obtained from the trial elastic stress tensor computed from the residual stress on which is applied a plastic correction. The elastic relation (9) is thus rewritten

$$\boldsymbol{\sigma}_{n+1}(\boldsymbol{x}) = \boldsymbol{\sigma}_n^{\mathrm{res}}(\boldsymbol{x}) + \mathbb{C}_i^{\mathrm{el}} : \Delta\boldsymbol{\varepsilon}_{n+1}^{\mathrm{r}}(\boldsymbol{x}) - \mathbb{C}_i^{\mathrm{el}} : \Delta p_{n+1}(\boldsymbol{x})\, \boldsymbol{N}_{n+1}(\boldsymbol{x}) \quad \forall \boldsymbol{x} \in \omega_i \,. \tag{16}$$

In this last equation, an implicit backward Euler integration was applied to the flow rule (8) and $\boldsymbol{N}$ is the plastic flow direction. In order to be able to obtain an isotropic residual-incremental-secant operator, the direction of the plastic flow is a first order approximation in $\Delta\boldsymbol{\varepsilon}$ –and not in $\Delta\boldsymbol{\varepsilon}^{\mathrm{r}}$– of the usual plastic flow (8) as discussed in [27], leading to

$$\boldsymbol{N}_{n+1}(\boldsymbol{x}) = \frac{3}{2}\frac{\mathbb{I}^{\mathrm{dev}} : (\boldsymbol{\sigma}_{n+1}(\boldsymbol{x}) - \boldsymbol{\sigma}_n^{\mathrm{res}}(\boldsymbol{x}))}{(\boldsymbol{\sigma}_{n+1}(\boldsymbol{x}) - \boldsymbol{\sigma}_n^{\mathrm{res}}(\boldsymbol{x}))^{\mathrm{eq}}} \,, \tag{17}$$

and which satisfies $\boldsymbol{N} : \boldsymbol{N} = \frac{3}{2}$. This problem can thus be solved on Δp in order to satisfy the yield criterion (6), *i.e.* $f(\boldsymbol{\sigma}_{n+1},\, p_{n+1} = p_n + \Delta p) = 0$.

The stress increment $\Delta\boldsymbol{\sigma}_{n+1}^{\mathrm{r}}$ evaluated from the residual state can thus be readily obtained following

$$\Delta\boldsymbol{\sigma}_{n+1}^{\mathrm{r}}(\boldsymbol{x}) = \mathbb{C}_i^{\mathrm{el}} : \Delta\boldsymbol{\varepsilon}_{n+1}^{\mathrm{r}}(\boldsymbol{x}) - 2\mu_i^{\mathrm{el}} \Delta p(\boldsymbol{x})\, \boldsymbol{N}_{n+1}(\boldsymbol{x}) = \mathbb{C}^{\mathrm{Sr}}(\boldsymbol{x}) : \Delta\boldsymbol{\varepsilon}_{n+1}^{\mathrm{r}}(\boldsymbol{x}) \,, \tag{18}$$

which allows computing the residual-incremental-secant operator $\mathbb{C}^{\mathrm{Sr}}(\boldsymbol{x})$. In the context of J2-plasticity, it was shown in [27] that $\mathbb{C}^{\mathrm{Sr}}(\boldsymbol{x})$ is an isotropic tensor

which can be expressed as

$$\mathbb{C}^{\mathrm{Sr}}(\boldsymbol{x}) = 3\kappa^{\mathrm{r}}(\boldsymbol{x})\,\mathbb{I}^{\mathrm{vol}} + 2\mu^{\mathrm{r}}(\boldsymbol{x})\,\mathbb{I}^{\mathrm{dev}} \quad \forall \boldsymbol{x} \in \omega_i\,, \tag{19}$$

with $\kappa^{\mathrm{r}}(\boldsymbol{x})$ and $\mu^{\mathrm{r}}(\boldsymbol{x})$ respectively the bulk and shear moduli of the equivalent isotropic-linear material, see details in [27].

3.2.2. Zero-incremental-secant approach

As previously mentioned, when defining the LCC during the MFH process, it can be necessary to modify the residual-incremental-secant approach by neglecting the residual stress -but not the residual strain- in the matrix phase. This modification is illustrated in Fig. 1(b) and consists in neglecting $\boldsymbol{\sigma}_n^{\mathrm{res}}$ in the formalism described here above, which leads to defining the zero-incremental-secant operator

$$\mathbb{C}^{\mathrm{S0}}(\boldsymbol{x}) = 3\kappa^{0}(\boldsymbol{x})\,\mathbb{I}^{\mathrm{vol}} + 2\mu^{0}(\boldsymbol{x})\,\mathbb{I}^{\mathrm{dev}} \quad \forall \boldsymbol{x} \in \omega_i\,. \tag{20}$$

Note that for this approach the plastic flow direction $\boldsymbol{N}$ corresponds strictly to the yield surface normal direction.

3.2.3. Non-local damage-enhanced incremental-secant approach

The incremental-secant approach can be extended to the case of elasto-plastic materials exhibiting damage. This has been done in [29] in the context of a Lemaitre-Chaboche damage model [30, 31] formulated in a non-local way [32–35]. The non-local formulation of the damage evolution is required in order to avoid the loss of the solution uniqueness at the structural level. In the context of a local damage model, this loss occurs at softening onset of the homogenised material law obtained by an incremental-secant MFH process.

3.3. *Residual-incremental-secant operator with second statistical moment estimations*

The volume averaging in the phase i of the stress expression (16) reads

$$\begin{aligned}
\bar{\boldsymbol{\sigma}}_{n+1} = \langle \boldsymbol{\sigma}_{n+1} \rangle &= \langle \mathbb{C}_i^{\mathrm{el}} : (\Delta\boldsymbol{\varepsilon}_{n+1}^{\mathrm{r}} - \Delta p_{n+1}\boldsymbol{N}_{n+1}) + \boldsymbol{\sigma}_n^{\mathrm{res}} \rangle \\
&= \mathbb{C}_i^{\mathrm{el}} : \langle \Delta\boldsymbol{\varepsilon}_{n+1}^{\mathrm{r}} \rangle - \mathbb{C}_i^{\mathrm{el}} : \langle \Delta p_{n+1}\boldsymbol{N}_{n+1} \rangle + \langle \boldsymbol{\sigma}_n^{\mathrm{res}} \rangle \\
&= \mathbb{C}_i^{\mathrm{el}} : \Delta\bar{\boldsymbol{\varepsilon}}_{n+1}^{\mathrm{r}} - \mathbb{C}_i^{\mathrm{el}} : \overline{(\Delta p_{n+1}\boldsymbol{N}_{n+1})} + \bar{\boldsymbol{\sigma}}_n^{\mathrm{res}} \quad \text{on } \omega_i\,.
\end{aligned} \tag{21}$$

Although the resulting macro stress and strain tensors are the first statistical moment volume averages of the respective local (micro) stress and strain tensors, the evolution of the local accumulated plastic strain increment Δp_{n+1} depends on the local von Mises stress (7) through Eq. (6). As the definition (7) involves quadratic terms, this suggests that more accurate results are expected if the second term on the right hand side of Eq. (21) is based on second statistical moment estimations of the stress field as proposed in [41]. In the following an incremental-secant predictor-corrector return mapping scheme with a second statistical moment estimation of the von Mises stress is developed in the phase ω_i. The residual form of this approach is first considered, while the zero-incremental-secant form will be deduced in the next subsection.

3.3.1. Elastic predictor

Let us consider an elasto-plastic material in phase i, which obeys J_2 elasto-plasticity. First it is assumed that the strain increment is elastic at each point of

the considered phase. A trial stress increment, which is also called elastic predictor $\Delta\boldsymbol{\sigma}^{\mathrm{tr}}$, is thus computed from the residual strain-stress state defined in Fig. 1(a) following

$$\Delta\boldsymbol{\sigma}^{\mathrm{tr}}_{n+1}(\boldsymbol{x}) = \mathbb{C}^{\mathrm{el}}_i : \Delta\boldsymbol{\varepsilon}^{\mathrm{r}}_{n+1}(\boldsymbol{x}) \quad \forall \boldsymbol{x} \in \omega_i \,, \tag{22}$$

with the elastic stress predictor

$$\boldsymbol{\sigma}^{\mathrm{tr}}_{n+1}(\boldsymbol{x}) = \boldsymbol{\sigma}^{\mathrm{res}}_{n}(\boldsymbol{x}) + \Delta\boldsymbol{\sigma}^{\mathrm{tr}}_{n+1}(\boldsymbol{x}) = \boldsymbol{\sigma}^{\mathrm{res}}_{n}(\boldsymbol{x}) + \mathbb{C}^{\mathrm{el}}_i : \Delta\boldsymbol{\varepsilon}^{\mathrm{r}}_{n+1}(\boldsymbol{x}) \quad \forall \boldsymbol{x} \in \omega_i \,. \tag{23}$$

During this elastic predictor step, the real composite material is replaced by a LCC with the same micro structure, and whose phases i have the elastic operators $\mathbb{C}^{\mathrm{el}}_i$ of the original phases. Applying the MFH scheme (1-3) with those elastic operators $\mathbb{C}^{\mathrm{el}}_i$ leads to the LCC elastic operator $\bar{\mathbb{C}}^{\mathrm{el}}$

$$\bar{\mathbb{C}}^{\mathrm{el}} = \left[v_{\mathrm{I}} \mathbb{C}^{\mathrm{el}}_{\mathrm{I}} : \mathbb{B}^{\epsilon} + v_0 \mathbb{C}^{\mathrm{el}}_0 \right] : \left[v_{\mathrm{I}} \mathbb{B}^{\epsilon} + v_0 \mathbb{I} \right]^{-1} , \text{ with} \tag{24}$$

$$\mathbb{B}^{\epsilon} = \{ \mathbb{I} + \mathbb{S} : [\left(\mathbb{C}^{\mathrm{el}}_0 \right)^{-1} : \mathbb{C}^{\mathrm{el}}_{\mathrm{I}} - \mathbb{I}] \}^{-1} \,. \tag{25}$$

Following the argumentation in [48, 49], the elastic predictor can be obtained in each phase from the second statistical moment estimation of the total strain, as

$$\langle \Delta\boldsymbol{\varepsilon}^{\mathrm{r}}_{n+1} \otimes \Delta\boldsymbol{\varepsilon}^{\mathrm{r}}_{n+1} \rangle_{\omega_i} = \frac{1}{v_i} \Delta\bar{\boldsymbol{\varepsilon}}^{\mathrm{r}}_{n+1} : \frac{\partial \bar{\mathbb{C}}^{\mathrm{el}}}{\partial \mathbb{C}^{\mathrm{el}}_i} : \Delta\bar{\boldsymbol{\varepsilon}}^{\mathrm{r}}_{n+1} \,, \tag{26}$$

where $\Delta\bar{\boldsymbol{\varepsilon}}^{\mathrm{r}}_{n+1}$ is the volume average of the composite material strain increment measured from its residual state. The second statistical moment estimation of the stress increment prediction can then be evaluated using Eqs. (4) and (5) as

$$\begin{aligned} \Delta\hat{\bar{\sigma}}^{\mathrm{tr}\,\mathrm{eq}}_{i\;n+1} &= \sqrt{\frac{3}{2} \mathbb{I}^{\mathrm{dev}} :: \langle \Delta\boldsymbol{\sigma}^{\mathrm{tr}}_{n+1} \otimes \Delta\boldsymbol{\sigma}^{\mathrm{tr}}_{n+1} \rangle_{\omega_i}} \\ &= 3\mu^{\mathrm{el}}_i \sqrt{\frac{2}{3} \mathbb{I}^{\mathrm{dev}} :: \langle \Delta\boldsymbol{\varepsilon}^{\mathrm{r}}_{n+1} \otimes \Delta\boldsymbol{\varepsilon}^{\mathrm{r}}_{n+1} \rangle_{\omega_i}} \,, \end{aligned} \tag{27}$$

with no sum on i intended. Note that $\Delta\hat{\bar{\sigma}}^{\mathrm{tr}\,\mathrm{eq}}_{i\;n+1}$ is not the equivalent von Mises stress of $\Delta\bar{\boldsymbol{\sigma}}^{\mathrm{tr}}_i$, *i.e.* $\Delta\hat{\bar{\sigma}}^{\mathrm{tr}\,\mathrm{eq}}_i \neq \sqrt{\frac{3}{2} \Delta\bar{\boldsymbol{\sigma}}^{\mathrm{tr}}_i : \mathbb{I}^{\mathrm{dev}} : \Delta\bar{\boldsymbol{\sigma}}^{\mathrm{tr}}_i}$. Similarly the following second statistical moment estimates can also be defined

$$\hat{\bar{\sigma}}^{\mathrm{res}\,\mathrm{eq}}_{i\;n} = \sqrt{\frac{3}{2} \mathbb{I}^{\mathrm{dev}} :: \langle \boldsymbol{\sigma}^{\mathrm{res}}_{n} \otimes \boldsymbol{\sigma}^{\mathrm{res}}_{n} \rangle_{\omega_i}} \,, \tag{28}$$

$$\hat{\bar{\sigma}}^{\mathrm{tr}\,\mathrm{eq}}_{i\;n+1} = \sqrt{\frac{3}{2} \mathbb{I}^{\mathrm{dev}} :: \langle \boldsymbol{\sigma}^{\mathrm{tr}}_{n+1} \otimes \boldsymbol{\sigma}^{\mathrm{tr}}_{n+1} \rangle_{\omega_i}} \,. \tag{29}$$

The first statistical moment predictor can be evaluated from the local field (23) as

$$\bar{\boldsymbol{\sigma}}^{\mathrm{tr}}_{i\;n+1} = \bar{\boldsymbol{\sigma}}^{\mathrm{res}}_{i\;n} + \Delta\bar{\boldsymbol{\sigma}}^{\mathrm{tr}}_{i\;n+1} = \bar{\boldsymbol{\sigma}}^{\mathrm{res}}_{n} + \mathbb{C}^{\mathrm{el}}_i : \Delta\bar{\boldsymbol{\varepsilon}}^{\mathrm{r}}_{i\;n+1} \,. \tag{30}$$

To evaluate the second statistical moment of the equivalent von Mises predictor (29), assumptions have to be made.

In the current context of the incremental-secant approach, we consider the approximation

$$\left\langle \boldsymbol{\sigma}_n^{\mathrm{res}} : \mathbb{I}^{\mathrm{dev}} : \Delta\boldsymbol{\sigma}_{n+1} \right\rangle_{\omega_i} \simeq \bar{\boldsymbol{\sigma}}_{i\,n}^{\mathrm{res}} : \mathbb{I}^{\mathrm{dev}} : \Delta\bar{\boldsymbol{\sigma}}_{i\,n+1} \ . \tag{31}$$

The two Eqs. (13) and (23) can be rewritten under the form

$$\begin{cases} \boldsymbol{\sigma}_n(\boldsymbol{x}) = \boldsymbol{\sigma}_n^{\mathrm{res}}(\boldsymbol{x}) + \Delta\boldsymbol{\sigma}_n^{\mathrm{unload}}(\boldsymbol{x}) & \forall \boldsymbol{x} \in \omega_i \, ; \\ \boldsymbol{\sigma}_{n+1}^{\mathrm{tr}}(\boldsymbol{x}) = \boldsymbol{\sigma}_n^{\mathrm{res}}(\boldsymbol{x}) + \Delta\boldsymbol{\sigma}_{n+1}^{\mathrm{tr}}(\boldsymbol{x}) & \forall \boldsymbol{x} \in \omega_i \ , \end{cases} \tag{32}$$

yielding the second statistical moment estimations in the phase i

$$\begin{cases} \left(\hat{\hat{\sigma}}_{i\ n}^{\mathrm{eq}}\right)^2 = \frac{3}{2}\left\langle \left(\boldsymbol{\sigma}_n^{\mathrm{res}}(\boldsymbol{x}) + \Delta\boldsymbol{\sigma}_n^{\mathrm{unload}}(\boldsymbol{x})\right) : \mathbb{I}^{\mathrm{dev}} : \left(\boldsymbol{\sigma}_n^{\mathrm{res}}(\boldsymbol{x}) + \Delta\boldsymbol{\sigma}_n^{\mathrm{unload}}(\boldsymbol{x})\right)\right\rangle_{\omega_i} \, ; \\ \left(\hat{\hat{\sigma}}_{i\ n+1}^{\mathrm{tr\,eq}}\right)^2 = \frac{3}{2}\left\langle \left(\boldsymbol{\sigma}_n^{\mathrm{res}}(\boldsymbol{x}) + \Delta\boldsymbol{\sigma}_{n+1}^{\mathrm{tr}}(\boldsymbol{x})\right) : \mathbb{I}^{\mathrm{dev}} : \left(\boldsymbol{\sigma}_n^{\mathrm{res}}(\boldsymbol{x}) + \Delta\boldsymbol{\sigma}_{n+1}^{\mathrm{tr}}(\boldsymbol{x})\right)\right\rangle_{\omega_i} \ . \end{cases} \tag{33}$$

Applying the assumption (31) on these two expressions leads to

$$\begin{cases} \left(\hat{\hat{\sigma}}_{i\ n}^{\mathrm{eq}}\right)^2 \simeq & \frac{3}{2}\left\langle \boldsymbol{\sigma}_n^{\mathrm{res}}(\boldsymbol{x}) : \mathbb{I}^{\mathrm{dev}} : \boldsymbol{\sigma}_n^{\mathrm{res}}(\boldsymbol{x})\right\rangle_{\omega_i} + 3\ \bar{\boldsymbol{\sigma}}_{i\ n}^{\mathrm{res}} : \mathbb{I}^{\mathrm{dev}} : \Delta\bar{\boldsymbol{\sigma}}_{i\ n}^{\mathrm{unload}} + \\ & \frac{3}{2}\left\langle \Delta\boldsymbol{\sigma}_n^{\mathrm{unload}}(\boldsymbol{x}) : \mathbb{I}^{\mathrm{dev}} : \Delta\boldsymbol{\sigma}_n^{\mathrm{unload}}(\boldsymbol{x})\right\rangle_{\omega_i} \, ; \\ \left(\hat{\hat{\sigma}}_{i\ n+1}^{\mathrm{tr\,eq}}\right)^2 \simeq & \frac{3}{2}\left\langle \boldsymbol{\sigma}_n^{\mathrm{res}}(\boldsymbol{x}) : \mathbb{I}^{\mathrm{dev}} : \boldsymbol{\sigma}_n^{\mathrm{res}}(\boldsymbol{x})\right\rangle_{\omega_i} + 3\ \bar{\boldsymbol{\sigma}}_{i\ n}^{\mathrm{res}} : \mathbb{I}^{\mathrm{dev}} : \Delta\bar{\boldsymbol{\sigma}}_{i\ n+1}^{\mathrm{tr}} + \\ & \frac{3}{2}\left\langle \Delta\boldsymbol{\sigma}_{n+1}^{\mathrm{tr}}(\boldsymbol{x}) : \mathbb{I}^{\mathrm{dev}} : \Delta\boldsymbol{\sigma}_{n+1}^{\mathrm{tr}}(\boldsymbol{x})\right\rangle_{\omega_i} \ . \end{cases} \tag{34}$$

The combination of these last two results directly yields the following approximation

$$\begin{aligned} \left(\hat{\hat{\sigma}}_{i\ n+1}^{\mathrm{tr\,eq}}\right)^2 \simeq \left(\hat{\hat{\sigma}}_{i\,n}^{\mathrm{eq}}\right)^2 - \left(\Delta\hat{\hat{\sigma}}_{i\ n+1}^{\mathrm{unload\,eq}}\right)^2 - 3\ \bar{\boldsymbol{\sigma}}_{i\ n}^{\mathrm{res}} : \mathbb{I}^{\mathrm{dev}} : \Delta\bar{\boldsymbol{\sigma}}_{i\ n}^{\mathrm{unload}} + \\ \left(\Delta\hat{\hat{\sigma}}_{i\ n+1}^{\mathrm{tr\,eq}}\right)^2 + 3\ \bar{\boldsymbol{\sigma}}_{i\ n}^{\mathrm{res}} : \mathbb{I}^{\mathrm{dev}} : \Delta\bar{\boldsymbol{\sigma}}_{i\ n+1}^{\mathrm{tr}} \ . \end{aligned} \tag{35}$$

In the context of a reloading reaching the same stress state, *i.e.* $\bar{\boldsymbol{\sigma}}_{i\,n+1} = \bar{\boldsymbol{\sigma}}_{i\,n}$, this equation leaves the second statistical moment estimation of the von Mises stress unchanged, *i.e.* $\hat{\hat{\sigma}}_{i\ n+1}^{\mathrm{tr\,eq}} = \hat{\hat{\sigma}}_{i\,n}^{\mathrm{eq}}$.

Practically, $\hat{\hat{\sigma}}_{i\,n}^{\mathrm{eq}}$ is a known value which was computed at the previous step, $\Delta\bar{\boldsymbol{\sigma}}_{i\ n}^{\mathrm{unload}}$ is computed during the unloading step, see next section, which allows to compute $\left(\Delta\hat{\hat{\sigma}}_{i\ n+1}^{\mathrm{unload\,eq}}\right)^2$ from (27) using the unloading increment as argument, the value $\Delta\hat{\hat{\sigma}}_{i\ n+1}^{\mathrm{tr\,eq}}$ is evaluated during the current time increment from (27), which eventually allows determining $\hat{\hat{\sigma}}_{i\ n+1}^{\mathrm{tr\,eq}}$ from (35).

One more time, $\hat{\hat{\sigma}}_{i\ n+1}^{\mathrm{tr\,eq}}$ is not equal to $\hat{\sigma}_{i\ n+1}^{\mathrm{tr\,eq}}$ the equivalent von Mises stress of $\bar{\boldsymbol{\sigma}}_{i\ n+1}^{\mathrm{tr}}$, which is used in the first statistical moment method, *i.e.*

$$\hat{\hat{\sigma}}_{i\ n+1}^{\mathrm{tr\,eq}} \neq \hat{\sigma}_{i\ n+1}^{\mathrm{tr\,eq}} = (\bar{\boldsymbol{\sigma}}_{i\ n+1}^{\mathrm{tr}})^{\mathrm{eq}} = \sqrt{\frac{3}{2}\bar{\boldsymbol{\sigma}}_{i\ n+1}^{\mathrm{tr}} : \mathbb{I}^{\mathrm{dev}} : \bar{\boldsymbol{\sigma}}_{i\ n+1}^{\mathrm{tr}}} \, . \tag{36}$$

The second statistical moment evaluation of the trial stress (35) can now be used

to evaluate the yield criterion (6), *i.e* in phase i

$$f = \hat{\bar{\sigma}}_i^{\mathrm{tr}\,\mathrm{eq}}{}_{n+1} - R(p_{in}) - \sigma_{\mathrm{Y}i} \leqslant 0\,. \tag{37}$$

On the one hand, if this condition is verified, the behaviour remains elastic, therefore:

$$\Delta\bar{\boldsymbol{\sigma}}_i^{\mathrm{r}}{}_{n+1} = \Delta\bar{\boldsymbol{\sigma}}_i^{\mathrm{tr}}{}_{n+1}\,, \quad \Delta\bar{\boldsymbol{\varepsilon}}_i^{\mathrm{p}}{}_{n+1} = \mathbf{0}\,, \text{ and } \Delta\bar{p}_{i\,n+1} = 0\,, \tag{38}$$

and the average stress at t_{n+1} is directly obtained from the trial stress

$$\bar{\boldsymbol{\sigma}}_{i\,n+1} = \bar{\boldsymbol{\sigma}}_i^{\mathrm{tr}}{}_{n+1}\,, \tag{39}$$

computed from Eq. (30) and the uniformly constructed secant operator of the phase i corresponds to the elastic operator,

$$\hat{\mathbb{C}}_i^{\mathrm{Sr}} = \mathbb{C}_i^{\mathrm{el}} = 3\kappa_i^{\mathrm{el}}\mathbb{I}^{\mathrm{vol}} + 2\mu_i^{\mathrm{el}}\mathbb{I}^{\mathrm{dev}}\,. \tag{40}$$

On the other hand, if the condition (37) is not verified, a plastic correction step is required.

3.3.2. Plastic corrections step

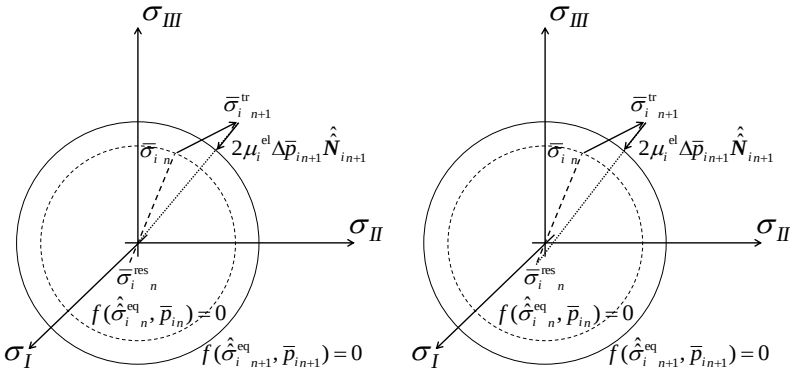

(a) Radial return mapping (b) Approximation

Figure 2. Plastic corrections illustration in the stress space using the second statistical moment estimation of the normal tensor. Figure adapted from [27]. (a) Radial return mapping; and (b) First-order approximation (42).

If condition (37) is not satisfied, the plastic flow has to be evaluated in the mean-field sense to correct the stress tensor. Equation (21) is rewritten in phase i as

$$\bar{\boldsymbol{\sigma}}_{i\,n+1} = \bar{\boldsymbol{\sigma}}_i^{\mathrm{tr}}{}_{n+1} - \mathbb{C}_i^{\mathrm{el}} : \Delta\bar{\boldsymbol{\varepsilon}}_i^{\mathrm{p}}{}_{n+1}\,, \quad \text{with} \quad \Delta\bar{\boldsymbol{\varepsilon}}_i^{\mathrm{p}}{}_{n+1} \approx \Delta\bar{p}_{i\,n+1}\,\hat{\hat{\boldsymbol{N}}}_{i\,n+1}\,, \tag{41}$$

with the plastic flow direction $\hat{\hat{\boldsymbol{N}}}_i$ constructed to be uniform on the phase i. This uniform plastic flow direction is constructed so that the yield condition respects the second statistical moments, see Fig. 2, but also to obtain an isotropic secant operator in order to perform the MFH without the isotropisation approximation.

In this work we consider the following direction for the return mapping

$$\hat{\hat{\boldsymbol{N}}}_{i\,n+1} = \frac{3}{2}\frac{\mathbb{I}^{\text{dev}} : \left(\bar{\boldsymbol{\sigma}}_{i\,n+1} - \bar{\boldsymbol{\sigma}}_{i}^{\text{res}}{}_{n}\right)}{\left(\bar{\boldsymbol{\sigma}}_{i\,n+1} - \bar{\boldsymbol{\sigma}}_{i}^{\text{res}}{}_{n}\right)^{\text{eq}}} = \frac{3}{2}\frac{\mathbb{I}^{\text{dev}} : \Delta\bar{\boldsymbol{\sigma}}_{i\,n+1}^{\text{r}}}{\Delta\hat{\bar{\sigma}}_{i\,n+1}^{\text{r}\,\text{eq}}}\,, \tag{42}$$

with, following Eq. (5),

$$\Delta\hat{\bar{\sigma}}_{i\,n+1}^{\text{r}\,\text{eq}} = \sqrt{\frac{3}{2}\mathbb{I}^{\text{dev}} :: \langle \Delta\boldsymbol{\sigma}_{n+1}^{\text{r}} \otimes \Delta\boldsymbol{\sigma}_{n+1}^{\text{r}} \rangle_{\omega_i}}\,, \tag{43}$$

When considering Eq. (42), it appears that the plastic correction is a first order approximation in $\Delta\bar{\boldsymbol{\varepsilon}}^{\text{p}}$ of the real normal to the yield surface as illustrated in Fig. 2(b). Indeed as the residual stress is not zero, the tensor $\hat{\hat{\boldsymbol{N}}}_i$ is normal to the yield surface only if the stress tensors and the residual stress are aligned. This approximation was discussed in [27].

3.3.2.1. Return mapping. Now we need to develop the plastic corrections part of the return mapping algorithm. First the normal direction obtained from the elastic predictor is introduced:

$$\hat{\hat{\boldsymbol{N}}}_{i}^{\text{tr}}{}_{n+1} = \frac{3}{2}\frac{\mathbb{I}^{\text{dev}} : \left(\bar{\boldsymbol{\sigma}}_{i}^{\text{tr}}{}_{n+1} - \bar{\boldsymbol{\sigma}}_{i}^{\text{res}}{}_{n}\right)}{\left(\bar{\boldsymbol{\sigma}}_{i}^{\text{tr}}{}_{n+1} - \bar{\boldsymbol{\sigma}}_{i}^{\text{res}}{}_{n}\right)^{\text{eq}}} = \frac{3}{2}\frac{\mathbb{I}^{\text{dev}} : \Delta\bar{\boldsymbol{\sigma}}_{i}^{\text{tr}}{}_{n+1}}{\Delta\hat{\bar{\sigma}}_{i}^{\text{tr}\,\text{eq}}{}_{n+1}}\,, \tag{44}$$

Since $\mathbb{C}_i^{\text{el}}$ is isotropic and $\Delta\bar{\boldsymbol{\varepsilon}}_i^{\text{p}}$ is deviatoric, Eq. (41) can be rewritten using (42) as

$$\mathbb{I}^{\text{dev}} : \bar{\boldsymbol{\sigma}}_{i\,n+1} = \mathbb{I}^{\text{dev}} : \bar{\boldsymbol{\sigma}}_{i}^{\text{tr}}{}_{n+1} - 2\mu_i^{\text{el}}\,\Delta\bar{p}_{i\,n+1}\,\hat{\hat{\boldsymbol{N}}}_{i\,n+1}\,. \tag{45}$$

Subtracting the residual stress $\bar{\boldsymbol{\sigma}}_{i}^{\text{res}}{}_{n}$ from both sides of Eq. (45),

$$\mathbb{I}^{\text{dev}} : (\bar{\boldsymbol{\sigma}}_{i\,n+1} - \bar{\boldsymbol{\sigma}}_{i}^{\text{res}}{}_{n}) = \mathbb{I}^{\text{dev}} : \left(\bar{\boldsymbol{\sigma}}_{i}^{\text{tr}}{}_{n+1} - \bar{\boldsymbol{\sigma}}_{i}^{\text{res}}{}_{n}\right) - 2\mu_i^{\text{el}}\,\Delta\bar{p}_{i\,n+1}\,\hat{\hat{\boldsymbol{N}}}_{i\,n+1} \tag{46}$$

and using both normal definitions (42) and (44), one has

$$\left(\Delta\hat{\bar{\sigma}}_{i\,n+1}^{\text{r}\,\text{eq}} + 3\mu_i^{\text{el}}\,\Delta\bar{p}_{i\,n+1}\right)\hat{\hat{\boldsymbol{N}}}_{i\,n+1} = \Delta\hat{\bar{\sigma}}_{i}^{\text{tr}\,\text{eq}}{}_{n+1}\,\hat{\hat{\boldsymbol{N}}}_{i}^{\text{tr}}{}_{n+1}\,. \tag{47}$$

Assuming that both normal tensors (42) and (44) have the same norm, *i.e.* $\hat{\hat{\boldsymbol{N}}}_i : \hat{\hat{\boldsymbol{N}}}_i = \hat{\hat{\boldsymbol{N}}}_i^{\text{tr}} : \hat{\hat{\boldsymbol{N}}}_i^{\text{tr}}$, this last relation implies

$$\hat{\hat{\boldsymbol{N}}}_{i\,n+1} = \hat{\hat{\boldsymbol{N}}}_{i}^{\text{tr}}{}_{n+1}\,, \quad \text{or} \quad \frac{\mathbb{I}^{\text{dev}} : \Delta\bar{\boldsymbol{\sigma}}_{i\,n+1}^{\text{r}}}{\Delta\hat{\bar{\sigma}}_{i\,n+1}^{\text{r}\,\text{eq}}} = \frac{\mathbb{I}^{\text{dev}} : \Delta\bar{\boldsymbol{\sigma}}_{i}^{\text{tr}}{}_{n+1}}{\Delta\hat{\bar{\sigma}}_{i}^{\text{tr}\,\text{eq}}{}_{n+1}}\,, \tag{48}$$

which, using the first statistical moment equivalent stress definition (36), leads to

$$\frac{\Delta\hat{\sigma}_{i\,n+1}^{\text{r}\,\text{eq}}}{\Delta\hat{\bar{\sigma}}_{i\,n+1}^{\text{r}\,\text{eq}}} = \frac{\Delta\hat{\sigma}_{i}^{\text{tr}\,\text{eq}}{}_{n+1}}{\Delta\hat{\bar{\sigma}}_{i}^{\text{tr}\,\text{eq}}{}_{n+1}}\,, \tag{49}$$

Eventually substituting (48) into (47) yields

$$\Delta\hat{\hat{\sigma}}_{i\,n+1}^{\mathrm{r}\,\mathrm{eq}} = \Delta\hat{\hat{\sigma}}_{i\,n+1}^{\mathrm{tr}\,\mathrm{eq}} - 3\mu_i^{\mathrm{el}}\,\Delta\bar{p}_{i\,n+1}\,. \tag{50}$$

Since a plastic flow occurred during the time interval $[t_n, t_{n+1}]$, the stress tensor at time t_{n+1} must satisfy the yield condition written in the second statistical moment sense, *i.e.*

$$f = \hat{\hat{\sigma}}_{i\,n+1}^{\mathrm{eq}} - R(\bar{p}_{i\,n+1}) - \sigma_{\mathrm{Y}_i} = 0\,. \tag{51}$$

In order to compute the value of $\hat{\hat{\sigma}}_{i\,n+1}^{\mathrm{eq}}$, the approximate relation (35) is rewritten for the final stress $\boldsymbol{\sigma}_{i\,n+1}$, and reads

$$\begin{aligned}\left(\hat{\hat{\sigma}}_{i\,n+1}^{\mathrm{eq}}\right)^2 \simeq \left(\hat{\hat{\sigma}}_{i\,n}^{\mathrm{eq}}\right)^2 - \left(\Delta\hat{\hat{\sigma}}_{i}^{\mathrm{unload}\,\mathrm{eq}}{}_{n+1}\right)^2 - 3\,\bar{\boldsymbol{\sigma}}_{i}^{\mathrm{res}}{}_{n} : \mathbb{I}^{\mathrm{dev}} : \Delta\bar{\boldsymbol{\sigma}}_{i}^{\mathrm{unload}}{}_{n} + \\ \left(\Delta\hat{\hat{\sigma}}_{i\,n+1}^{\mathrm{r}\,\mathrm{eq}}\right)^2 + 3\,\bar{\boldsymbol{\sigma}}_{i}^{\mathrm{res}}{}_{n} : \mathbb{I}^{\mathrm{dev}} : \Delta\bar{\boldsymbol{\sigma}}_{i\,n+1}^{\mathrm{r}}\,.\end{aligned} \tag{52}$$

Therefore, using equations (45) and (50), the yielding condition (51) becomes

$$\begin{aligned}\left(R\left(\bar{p}_{i\,n+1}\right) + \sigma_{\mathrm{Y}_i}\right)^2 &= \left(\hat{\hat{\sigma}}_{i\,n+1}^{\mathrm{eq}}\right)^2 \\ &= \left(\hat{\hat{\sigma}}_{i\,n}^{\mathrm{eq}}\right)^2 - \left(\Delta\hat{\hat{\sigma}}_{i}^{\mathrm{unload}\,\mathrm{eq}}{}_{n+1}\right)^2 - \\ &\quad 3\,\bar{\boldsymbol{\sigma}}_{i}^{\mathrm{res}}{}_{n} : \mathbb{I}^{\mathrm{dev}} : \Delta\bar{\boldsymbol{\sigma}}_{i}^{\mathrm{unload}}{}_{n} + \\ &\quad \left(\Delta\hat{\hat{\sigma}}_{i}^{\mathrm{tr}\,\mathrm{eq}}{}_{n+1} - 3\mu_i^{\mathrm{el}}\,\Delta\bar{p}_{i\,n+1}\right)^2 + \\ &\quad 3\,\bar{\boldsymbol{\sigma}}_{i}^{\mathrm{res}}{}_{n} : \mathbb{I}^{\mathrm{dev}} : \Delta\bar{\boldsymbol{\sigma}}_{i}^{\mathrm{tr}}{}_{n+1} - \\ &\quad 6\mu_i^{\mathrm{el}}\,\Delta\bar{p}_{i\,n+1}\,\bar{\boldsymbol{\sigma}}_{i}^{\mathrm{res}}{}_{n} : \mathbb{I}^{\mathrm{dev}} : \hat{\hat{\boldsymbol{N}}}_{i}^{\mathrm{tr}}{}_{n+1}\,.\end{aligned} \tag{53}$$

Note that in this equation we did not use the relation $\hat{\hat{\boldsymbol{N}}}_i^{\mathrm{tr}} : \hat{\hat{\boldsymbol{N}}}_i^{\mathrm{tr}} = \frac{3}{2}$ as this is usually not the case with the second statistical moments

This last equation in the accumulated plastic strain increment, $\Delta\bar{p}_{i\,n+1}$, is stated in the mean-field sense with second statistical moment estimations and can be solved numerically to fully define the plastic correction step.

3.3.2.2. Residual-incremental-secant operator. Once the stress tensor $\bar{\boldsymbol{\sigma}}_i$ at time t_{n+1} has been obtained from the return mapping algorithm, the residual-incremental-secant operator of the linear comparison material can be obtained as follows. Rewriting (14) and (15) in the mean-field sense in phase i yields

$$\bar{\boldsymbol{\sigma}}_{i\,n+1} = \bar{\boldsymbol{\sigma}}_{i}^{\mathrm{res}}{}_{n} + \Delta\bar{\boldsymbol{\sigma}}_{i\,n+1}^{\mathrm{r}}\,, \tag{54}$$

with

$$\Delta\bar{\boldsymbol{\sigma}}_{i\,n+1}^{\mathrm{r}} = \hat{\mathbb{C}}_{i}^{\mathrm{Sr}}{}_{n+1} : \Delta\bar{\boldsymbol{\varepsilon}}_{i\,n+1}^{\mathrm{r}}\,, \tag{55}$$

where $\hat{\mathbb{C}}_i^{\mathrm{Sr}}$ is the residual-incremental-secant operator of the linear comparison material, which is constructed to be uniform.

Using Eqs. (30), (41) and (45), Eq. (55) becomes

$$\Delta\bar{\boldsymbol{\sigma}}^{\mathrm{r}}_{i\,n+1} = \hat{\mathbb{C}}^{\mathrm{Sr}}_{i\;n+1} : \Delta\bar{\boldsymbol{\varepsilon}}^{\mathrm{r}}_{i\,n+1} = \mathbb{C}^{\mathrm{el}}_{i} : \Delta\bar{\boldsymbol{\varepsilon}}^{\mathrm{r}}_{i\,n+1} - 2\mu^{\mathrm{el}}_{i}\,\Delta\bar{p}_{i\,n+1}\,\hat{\hat{\boldsymbol{N}}}_{i\,n+1}\,, \tag{56}$$

which becomes after using (44) and (48),

$$\Delta\bar{\boldsymbol{\sigma}}^{\mathrm{r}}_{i\,n+1} = \left[\mathbb{C}^{\mathrm{el}}_{i} - 3\mu^{\mathrm{el}}_{i}\,\Delta\bar{p}_{i\,n+1}\,\frac{\mathbb{I}^{\mathrm{dev}} : \mathbb{C}^{\mathrm{el}}_{i}}{\Delta\hat{\bar{\sigma}}^{\mathrm{tr}\;\mathrm{eq}}_{i\;\;n+1}}\right] : \Delta\bar{\boldsymbol{\varepsilon}}^{\mathrm{r}}_{i\,n+1} = \hat{\mathbb{C}}^{\mathrm{Sr}}_{i\;n+1} : \Delta\bar{\boldsymbol{\varepsilon}}^{\mathrm{r}}_{i\,n+1}\,. \tag{57}$$

As it can be seen from this equation, for J2-elasto-plastic materials, since $\mathbb{C}^{\mathrm{el}}_{i}$ is isotropic the residual-incremental-secant operator of phase i of the linear comparison material $\hat{\mathbb{C}}^{\mathrm{Sr}}_{i}$ is also isotropic. Moreover, as $\mathbb{C}^{\mathrm{el}}_{i} = 3\kappa^{\mathrm{el}}_{i}\mathbb{I}^{\mathrm{vol}} + 2\mu^{\mathrm{el}}_{i}\mathbb{I}^{\mathrm{dev}}$, one can directly deduce

$$\hat{\mathbb{C}}^{\mathrm{Sr}}_{i\;n+1} = 3\,\hat{\kappa}^{\mathrm{r}}_{i\,n+1}\,\mathbb{I}^{\mathrm{vol}} + 2\,\hat{\mu}^{\mathrm{r}}_{i\,n+1}\,\mathbb{I}^{\mathrm{dev}}\,, \tag{58}$$

with

$$\hat{\kappa}^{\mathrm{r}}_{i\,n+1} = \kappa^{\mathrm{el}}_{i}, \quad \text{and} \tag{59}$$

$$\hat{\mu}^{\mathrm{r}}_{i\,n+1} = \mu^{\mathrm{el}}_{i} - \frac{3{\mu^{\mathrm{el}}_{i}}^{2}\,\Delta\bar{p}_{i\,n+1}}{\Delta\hat{\bar{\sigma}}^{\mathrm{tr}\;\mathrm{eq}}_{i\;\;n+1}}\,. \tag{60}$$

According to Eq. (27), this last result can also be rewritten as

$$\hat{\mu}^{\mathrm{r}}_{i\,n+1} = \mu^{\mathrm{el}}_{i}\left(1 - \frac{\Delta\bar{p}_{i\,n+1}}{\Delta\hat{\bar{\varepsilon}}^{\mathrm{r}\;\mathrm{eq}}_{i\;\;n+1}}\right)\,. \tag{61}$$

3.4. *Zero-incremental-secant operator with second statistical moment estimations*

With a view to MFH, it was shown in [27] that to accurately capture the elasto-plastic behaviour of the matrix phase when the matrix residual stress is located on the other side of the origin than the current stress state, the secant approach has to be applied in the matrix phase from a fictitious unloaded state corresponding to a residual strain for a stress state sets to zero, as illustrated in Fig. 1(b). This assumption consists in neglecting $\boldsymbol{\sigma}^{\mathrm{res}}_{n}$ in the second statistical moment residual-incremental formalism described in Section 3.3.

Similar results are straightforwardly obtained and can be summarised as follows. The stress tensor in mean-field sense in phase i reads

$$\bar{\boldsymbol{\sigma}}_{i\,n+1} = \Delta\bar{\boldsymbol{\sigma}}^{\mathrm{r}}_{i\,n+1}\,, \tag{62}$$

with

$$\Delta\bar{\boldsymbol{\sigma}}^{\mathrm{r}}_{i\,n+1} = \hat{\mathbb{C}}^{\mathrm{S0}}_{i\;n+1} : \Delta\bar{\boldsymbol{\varepsilon}}^{\mathrm{r}}_{i\,n+1}\,, \tag{63}$$

where $\hat{\mathbb{C}}^{\mathrm{S0}}_{i}$ is the zero-incremental-secant operator of the linear comparison material, which is constructed to be uniform. This operator reads

$$\hat{\mathbb{C}}^{\mathrm{S0}}_{i\;n+1} = 3\,\hat{\kappa}^{0}_{i\,n+1}\,\mathbb{I}^{\mathrm{vol}} + 2\,\hat{\mu}^{0}_{i\,n+1}\,\mathbb{I}^{\mathrm{dev}}\,, \tag{64}$$

with

$$\hat{\kappa}^{0}_{i\,n+1} = \kappa^{\mathrm{el}}_{i}, \quad \text{and} \tag{65}$$

$$\hat{\mu}^{0}_{i\,n+1} = \mu^{\mathrm{el}}_{i} - \frac{3{\mu^{\mathrm{el}}_{i}}^{2}\,\Delta\bar{p}_{i\,n+1}}{\Delta\hat{\bar{\sigma}}^{\mathrm{tr}\,\mathrm{eq}}_{i\;n+1}} = \mu^{\mathrm{el}}_{i}\left(1 - \frac{\Delta\bar{p}_{i\,n+1}}{\Delta\hat{\bar{\varepsilon}}^{\mathrm{r}\,\mathrm{eq}}_{i\;n+1}}\right). \tag{66}$$

A couple of remarks can be drawn at this moment.

- As the residual stress is neglected in this formalism, the second statistical moment estimations of the von Mises predictor (35) and of the current yield stress (53), are assumed to read

$$\left(\hat{\bar{\sigma}}^{\mathrm{tr}\,\mathrm{eq}}_{i\;n+1}\right)^2 = \left(\Delta\hat{\bar{\sigma}}^{\mathrm{tr}\,\mathrm{eq}}_{i\;n+1}\right)^2. \tag{67}$$

and to

$$\begin{aligned}\left(R\left(\bar{p}_{i\,n+1}\right) + \sigma_{\mathrm{Y}_i}\right)^2 &= \left(\hat{\bar{\sigma}}^{\mathrm{eq}}_{i\;n+1}\right)^2 \\ &= \left(\Delta\hat{\bar{\sigma}}^{\mathrm{tr}\,\mathrm{eq}}_{i\;n+1} - 3\mu^{\mathrm{el}}_{i}\,\Delta\bar{p}_{i\,n+1}\right)^2,\end{aligned} \tag{68}$$

without requiring the approximation (31).
- The return mapping direction (44) is rigorously the radial return mapping direction instead of being a first order approximation.

In the following $\hat{\mathbb{C}}^{\mathrm{S}}_{i\;n+1}$ will be used to either design $\hat{\mathbb{C}}^{\mathrm{Sr}}_{i\;n+1}$ or $\hat{\mathbb{C}}^{\mathrm{S0}}_{i\;n+1}$ depending on the considered method. Similarly, the bulk and shear moduli of the LCC phase i, $\hat{\kappa}_{i\,n+1}$ and $\hat{\mu}_{i\,n+1}$, either hold for $\hat{\kappa}^{\mathrm{r}}_{i\,n+1}$ and $\hat{\mu}^{\mathrm{r}}_{i\,n+1}$ or for $\hat{\kappa}^{0}_{i\,n+1}$ and $\hat{\mu}^{0}_{i\,n+1}$.

3.5. *"Consistent" algorithmic operators*

With a view toward the MFH resolution of the problem the "consistent" algorithmic operators of the incremental-secant method with second statistical moment estimations are required.

From Eqs. (54-55) and (62-63), the stress tensor is rewritten

$$\bar{\boldsymbol{\sigma}}_{i\,n+1} = \begin{cases} \bar{\boldsymbol{\sigma}}^{\mathrm{res}}_{i\;n} + \hat{\mathbb{C}}^{\mathrm{Sr}}_{i\;n+1} : \Delta\bar{\boldsymbol{\varepsilon}}^{\mathrm{r}}_{i\,n+1}\ ; \\ \hat{\mathbb{C}}^{\mathrm{S0}}_{i\;n+1} : \Delta\bar{\boldsymbol{\varepsilon}}^{\mathrm{r}}_{i\,n+1}\ , \end{cases} \tag{69}$$

for respectively the residual- and zero-incremental-secant methods.

The "consistent" algorithm operator can thus be expressed as[1]

$$\mathbb{C}^{\mathrm{algo}}_{i\;n+1} = \frac{\partial\,\bar{\boldsymbol{\sigma}}_{i\,n+1}}{\partial\bar{\boldsymbol{\varepsilon}}_{i}} = \hat{\mathbb{C}}^{\mathrm{S}}_{i\;n+1} + \Delta\,\bar{\boldsymbol{\varepsilon}}^{\mathrm{r}}_{i\,n+1} : \frac{\partial\,\hat{\mathbb{C}}^{\mathrm{S}}_{i\;n+1}}{\partial\bar{\boldsymbol{\varepsilon}}^{\mathrm{r}}_{i}}. \tag{70}$$

Moreover in this proposed second statistical moment MFH method, as $\hat{\bar{\varepsilon}}^{\mathrm{r}\,\mathrm{eq}}_{i\,n+1}$ is computed from Eqs. (26-27), it does not depend on the strain increment $\bar{\boldsymbol{\varepsilon}}^{\mathrm{r}}_{i}$ only,

[1]Note that $\frac{\partial}{\partial\bar{\boldsymbol{\varepsilon}}_i} = \frac{\partial}{\partial\Delta\bar{\boldsymbol{\varepsilon}}_i} = \frac{\partial}{\partial\Delta\bar{\boldsymbol{\varepsilon}}^{\mathrm{r}}_i}$

but it also depends explicitly on the strain increment of the composite material, and so for the operator $\hat{\mathbb{C}}_i^{\mathrm{S}}$. A complementary algorithmic operator is thus required:

$$\mathbb{C}_{ic}^{\mathrm{algo}}{}_{n+1} = \frac{\partial\, \bar{\boldsymbol{\sigma}}_{i\,n+1}}{\partial \bar{\boldsymbol{\varepsilon}}} = \Delta\, \bar{\boldsymbol{\varepsilon}}_{i\,n+1}^{\mathrm{r}} : \frac{\partial\, \hat{\mathbb{C}}_{i\,n+1}^{\mathrm{S}}}{\partial \bar{\boldsymbol{\varepsilon}}^{\mathrm{r}}}\,. \tag{71}$$

The expressions of the derivatives of $\hat{\mathbb{C}}_{i\,n+1}^{\mathrm{S}}$ with respect to $\bar{\boldsymbol{\varepsilon}}_i^{\mathrm{r}}$ and $\bar{\boldsymbol{\varepsilon}}^{\mathrm{r}}$ are reported in Appendix A.1.

4. Incremental-secant MFH with second statistical moment estimations

In this paper we consider a two-phase composite material. Considering a time interval $[t_n,\ t_{n+1}]$, the strain increment $\Delta\bar{\boldsymbol{\varepsilon}}_{n+1}$ resulting from the iterations at the weak form level is different from the strain increment $\Delta\bar{\boldsymbol{\varepsilon}}_{n+1}^{\mathrm{r}}$ applied to the LCC used in the MFH procedure. Combining (11) and (12) for the homogenised material leads to

$$\Delta\bar{\boldsymbol{\varepsilon}}_{n+1}^{\mathrm{r}} = \bar{\boldsymbol{\varepsilon}}_n + \Delta\bar{\boldsymbol{\varepsilon}}_{n+1} - \bar{\boldsymbol{\varepsilon}}_n^{\mathrm{res}}\,. \tag{72}$$

The residual variables follow from the application of a virtual elastic unloading step at time t_n canceling the stress in the composite material, *i.e.*

$$\bar{\boldsymbol{\sigma}}_n^{\mathrm{res}} = v_0\, \bar{\boldsymbol{\sigma}}_0^{\mathrm{res}}{}_n + v_{\mathrm{I}}\, \bar{\boldsymbol{\sigma}}_{\mathrm{I}}^{\mathrm{res}}{}_n = 0\,. \tag{73}$$

This virtual elastic unloading step is defined as follows:

- The unloading operator of the composite material is the elastic operator (24).
- The residual strain of the composite material satisfying $\bar{\boldsymbol{\sigma}}_n^{\mathrm{res}} = 0$ is directly obtained from

$$\bar{\boldsymbol{\varepsilon}}_n^{\mathrm{res}} = \bar{\boldsymbol{\varepsilon}}_n - \Delta\bar{\boldsymbol{\varepsilon}}_n^{\mathrm{unload}} = \bar{\boldsymbol{\varepsilon}}_n - (\bar{\mathbb{C}}^{\mathrm{el}})^{-1} : \bar{\boldsymbol{\sigma}}_{n+1}\,. \tag{74}$$

- Applying the MFH equations (1-3) in combination with this last result yields the residual states, in the mean-field sense, in the different phases

$$\bar{\boldsymbol{\varepsilon}}_{\mathrm{I}}^{\mathrm{res}}{}_n = \bar{\boldsymbol{\varepsilon}}_{\mathrm{I}\,n} - \mathbb{B}^{\epsilon} : [v_{\mathrm{I}}\mathbb{B}^{\epsilon} + v_0\mathbb{I}]^{-1} : \Delta\bar{\boldsymbol{\varepsilon}}_n^{\mathrm{unload}}\,, \tag{75}$$

$$\bar{\boldsymbol{\sigma}}_{\mathrm{I}}^{\mathrm{res}}{}_n = \bar{\boldsymbol{\sigma}}_{\mathrm{I}\,n} - \mathbb{C}_{\mathrm{I}}^{\mathrm{el}} : \mathbb{B}^{\epsilon} : [v_{\mathrm{I}}\mathbb{B}^{\epsilon} + v_0\mathbb{I}]^{-1} : \Delta\bar{\boldsymbol{\varepsilon}}_n^{\mathrm{unload}}\,, \tag{76}$$

$$\bar{\boldsymbol{\varepsilon}}_0^{\mathrm{res}}{}_n = \bar{\boldsymbol{\varepsilon}}_{0\,n} - [v_{\mathrm{I}}\mathbb{B}^{\epsilon} + v_0\mathbb{I}]^{-1} : \Delta\bar{\boldsymbol{\varepsilon}}_n^{\mathrm{unload}}\,, \text{ and} \tag{77}$$

$$\bar{\boldsymbol{\sigma}}_0^{\mathrm{res}}{}_n = \bar{\boldsymbol{\sigma}}_{0\,n} - \mathbb{C}_0^{\mathrm{el}} : [v_{\mathrm{I}}\mathbb{B}^{\epsilon} + v_0\mathbb{I}]^{-1} : \Delta\bar{\boldsymbol{\varepsilon}}_n^{\mathrm{unload}}\,. \tag{78}$$

Once the unloaded state is defined, considering a time interval $[t_n,\ t_{n+1}]$, the new stress state can be computed from the macro-total strain tensor $\bar{\boldsymbol{\varepsilon}}_n$, the secant strain increment $\Delta\bar{\boldsymbol{\varepsilon}}_{n+1}^{\mathrm{r}}$, and the phase i internal variables η_i at t_n completed by the residual variables (the residual strains in the composite material, in the fibres phase, and in the matrix phase). The incremental-secant MFH consists in rewriting

the Eqs. (1-3) using the secant operators (69) and Eq. (73), which results into

$$\Delta\bar{\boldsymbol{\varepsilon}}^{\mathrm{r}}_{n+1} = v_0 \Delta\boldsymbol{\varepsilon}_0{}^{\mathrm{r}}_{n+1} + v_{\mathrm{I}} \Delta\boldsymbol{\varepsilon}_{\mathrm{I}}{}^{\mathrm{r}}_{n+1} \,, \tag{79}$$

$$\bar{\boldsymbol{\sigma}}_{n+1} = v_0 \; \bar{\boldsymbol{\sigma}}_{0\,n+1} + v_{\mathrm{I}} \; \bar{\boldsymbol{\sigma}}_{\mathrm{I}\,n+1} = v_0 \; \Delta\bar{\boldsymbol{\sigma}}^{\mathrm{r}}_{0\,n+1} + v_{\mathrm{I}} \; \Delta\bar{\boldsymbol{\sigma}}^{\mathrm{r}}_{\mathrm{I}\,n+1} \;, \tag{80}$$

$$\Delta\bar{\boldsymbol{\varepsilon}}^{\mathrm{r}}_{\mathrm{I}\,n+1} = \mathbb{B}^{\epsilon}\left(\mathrm{I}, \hat{\mathbb{C}}^{\mathrm{S}}_0, \hat{\mathbb{C}}^{\mathrm{S}}_{\mathrm{I}}\right) : \Delta\bar{\boldsymbol{\varepsilon}}^{\mathrm{r}}_{0\,n+1} \;. \tag{81}$$

In this formalism, the stress increments $\Delta\bar{\boldsymbol{\sigma}}^{\mathrm{r}}_{i\,n+1}$ and secant operator $\hat{\mathbb{C}}^{\mathrm{Sr}}_i$ in phase i are evaluated from $\Delta\bar{\boldsymbol{\varepsilon}}^{\mathrm{r}}_{i\,n+1}$ and from $\Delta\bar{\boldsymbol{\varepsilon}}^{\mathrm{r}}_{n+1}$ using the second statistical moment-enhanced elasto-plastic material model described in Section 3.3, with

$$\bar{\boldsymbol{\sigma}}_{i\,n+1} = \mathcal{F}_i\left(\Delta\bar{\boldsymbol{\varepsilon}}^{\mathrm{r}}_{i\,n+1}\,,\; \Delta\bar{\boldsymbol{\varepsilon}}^{\mathrm{r}}{}_{n+1}\,;\, \eta_{in},\; \bar{\boldsymbol{\varepsilon}}^{\mathrm{res}}_i{}_{n}\,,\; \bar{\boldsymbol{\sigma}}^{\mathrm{res}}_i{}_{n}\right) \,, \tag{82}$$

and

$$\hat{\mathbb{C}}^{\mathrm{S}}_{r\,n+1} = \mathcal{G}_i\left(\Delta\bar{\boldsymbol{\varepsilon}}^{\mathrm{r}}_{i\,n+1}\,,\; \Delta\bar{\boldsymbol{\varepsilon}}^{\mathrm{r}}{}_{n+1}\,;\, \eta_{in},\; \bar{\boldsymbol{\varepsilon}}^{\mathrm{res}}_i{}_{n}\,,\; \bar{\boldsymbol{\sigma}}^{\mathrm{res}}_i{}_{n}\right) \,. \tag{83}$$

Finally, in order to perform Newton-Raphson iterations at the finite-element level, the linearisation of the homogenised stress (80) has to be performed. Using Eqs. (70) and (71), one has

$$\begin{aligned}
\delta\bar{\boldsymbol{\sigma}} = {} & v_{\mathrm{I}}\left(\frac{\partial\,\bar{\boldsymbol{\sigma}}_{\mathrm{I}\,n+1}}{\partial\Delta\bar{\boldsymbol{\varepsilon}}^{\mathrm{r}}_{\mathrm{I}}} : \delta\Delta\bar{\boldsymbol{\varepsilon}}^{\mathrm{r}}_{\mathrm{I}} + \frac{\partial\,\bar{\boldsymbol{\sigma}}_{\mathrm{I}\,n+1}}{\partial\Delta\bar{\boldsymbol{\varepsilon}}^{\mathrm{r}}} : \delta\Delta\bar{\boldsymbol{\varepsilon}}^{\mathrm{r}}\right) + \\
& v_0\left(\frac{\partial\,\bar{\boldsymbol{\sigma}}_{0\,n+1}}{\partial\Delta\bar{\boldsymbol{\varepsilon}}^{\mathrm{r}}_{0}} : \delta\Delta\bar{\boldsymbol{\varepsilon}}^{\mathrm{r}}_{0} + \frac{\partial\,\bar{\boldsymbol{\sigma}}_{0\,n+1}}{\partial\Delta\bar{\boldsymbol{\varepsilon}}^{\mathrm{r}}} : \delta\Delta\bar{\boldsymbol{\varepsilon}}^{\mathrm{r}}\right) \\
= {} & v_{\mathrm{I}}\left(\mathbb{C}^{\mathrm{algo}}_{\mathrm{I}\;n+1} : \delta\Delta\bar{\boldsymbol{\varepsilon}}^{\mathrm{r}}_{\mathrm{I}} + \mathbb{C}^{\mathrm{algo}}_{\mathrm{Ic}\;n+1} : \delta\Delta\bar{\boldsymbol{\varepsilon}}^{\mathrm{r}}\right) + \\
& v_0\left(\mathbb{C}^{\mathrm{algo}}_{0\;n+1} : \delta\Delta\bar{\boldsymbol{\varepsilon}}^{\mathrm{r}}_{0} + \mathbb{C}^{\mathrm{algo}}_{0\mathrm{c}\;n+1} : \delta\Delta\bar{\boldsymbol{\varepsilon}}^{\mathrm{r}}\right) \\
= {} & \left(v_{\mathrm{I}}\;\mathbb{C}^{\mathrm{algo}}_{\mathrm{I}\;n+1} : \frac{\partial\bar{\boldsymbol{\varepsilon}}_{\mathrm{I}}}{\partial\bar{\boldsymbol{\varepsilon}}} + v_{\mathrm{I}}\;\mathbb{C}^{\mathrm{algo}}_{\mathrm{Ic}\;n+1} + \right. \\
& \left. v_0\;\mathbb{C}^{\mathrm{algo}}_{0\;n+1} : \frac{\partial\bar{\boldsymbol{\varepsilon}}_{0}}{\partial\bar{\boldsymbol{\varepsilon}}} + v_0\;\mathbb{C}^{\mathrm{algo}}_{0\mathrm{c}\;n+1}\right) : \delta\bar{\boldsymbol{\varepsilon}}\,,
\end{aligned} \tag{84}$$

which allows defining the composite material "consistent" material operator

$$\begin{aligned}
\mathbb{C}^{\mathrm{algo}}{}_{n+1} = {} & \left(v_{\mathrm{I}}\;\mathbb{C}^{\mathrm{algo}}_{\mathrm{I}\;n+1} : \frac{\partial\bar{\boldsymbol{\varepsilon}}_{\mathrm{I}}}{\partial\bar{\boldsymbol{\varepsilon}}} + v_{\mathrm{I}}\;\mathbb{C}^{\mathrm{algo}}_{\mathrm{Ic}\;n+1} + \right. \\
& \left. v_0\;\mathbb{C}^{\mathrm{algo}}_{0\;n+1} : \frac{\partial\bar{\boldsymbol{\varepsilon}}_{0}}{\partial\bar{\boldsymbol{\varepsilon}}} + v_0\;\mathbb{C}^{\mathrm{algo}}_{0\mathrm{c}\;n+1}\right) \,.
\end{aligned} \tag{85}$$

The two terms $\frac{\partial\bar{\boldsymbol{\varepsilon}}_{\mathrm{I}}}{\partial\bar{\boldsymbol{\varepsilon}}}$ and $\frac{\partial\bar{\boldsymbol{\varepsilon}}_{\mathrm{I}}}{\partial\bar{\boldsymbol{\varepsilon}}}$are obtained during the MFH resolution.

Practically, for the Mori-Tanaka (M–T) model extended to the present formulation, the system of equations (79-83) is solved using the M-T process described here below.

- The strain increment in the inclusions phase is predicted as $\Delta\bar{\boldsymbol{\varepsilon}}^{\mathrm{r}}_{n+1} \rightarrow \Delta\bar{\boldsymbol{\varepsilon}}^{\mathrm{r}}_{\mathrm{I}\,n+1}$.
- A Newton-Raphson iterations process is then applied (indices related to the iteration number at time t_{n+1} are omitted):

(1) The average strain in the matrix phase is computed from:

$$\Delta\bar{\boldsymbol{\varepsilon}}^{\mathrm{r}}_{0\,n+1} = \frac{1}{v_0}\left(\Delta\bar{\boldsymbol{\varepsilon}}^{\mathrm{r}}_{n+1} - v_{\mathrm{I}}\,\Delta\bar{\boldsymbol{\varepsilon}}^{\mathrm{r}}_{\mathrm{I}\,n+1}\right) . \tag{86}$$

(2) For each phase i, call the second statistical moment-enhanced elasto-plastic constitutive model (82) described in Section 3.3. This constitutive law is now summarised.
The trial stress tensor is first evaluated from Eq. (30) as

$$\bar{\boldsymbol{\sigma}}^{\mathrm{tr}}_{i\;n+1} = \bar{\boldsymbol{\sigma}}^{\mathrm{res}}_{i\;n} + \Delta\bar{\boldsymbol{\sigma}}^{\mathrm{tr}}_{i\;n+1} = \bar{\boldsymbol{\sigma}}^{\mathrm{res}}_{n} + \mathbb{C}^{\mathrm{el}}_{i} : \Delta\bar{\boldsymbol{\varepsilon}}^{\mathrm{r}}_{n+1} , \tag{87}$$

for the residual-incremental-secant method or as

$$\bar{\boldsymbol{\sigma}}^{\mathrm{tr}}_{i\;n+1} = \Delta\bar{\boldsymbol{\sigma}}^{\mathrm{tr}}_{i\;n+1} = \mathbb{C}^{\mathrm{el}}_{i} : \Delta\bar{\boldsymbol{\varepsilon}}^{\mathrm{r}}_{n+1} , \tag{88}$$

for the zero-incremental-secant method.
Second, the second statistical moment estimation of the stress increment prediction is evaluated from Eq. (27). Note that in the inclusion phase this expression also corresponds to the first statistical moment prediction, *i.e.* $\Delta\hat{\bar{\sigma}}^{\mathrm{tr}\,\mathrm{eq}}_{\mathrm{I}} = \Delta\hat{\sigma}^{\mathrm{tr}\,\mathrm{eq}}_{\mathrm{I}} = (\Delta\bar{\boldsymbol{\sigma}}^{\mathrm{tr}}_{\mathrm{I}})^{\mathrm{eq}} = \sqrt{\frac{3}{2}\Delta\bar{\boldsymbol{\sigma}}^{\mathrm{tr}}_{\mathrm{I}} : \mathbb{I}^{\mathrm{dev}} : \Delta\bar{\boldsymbol{\sigma}}^{\mathrm{tr}}_{\mathrm{I}}}$ for a M-T scheme (25). The first statistical moment residual-incremental-secant approach described in Section 3.2.1 is thus used in the inclusion phase.
Third, the second statistical moment estimation of von Mises elastic predictor is obtained from either the approximation (35) or from the approximation (67) for the residual- and zero-incremental-secant formulations, respectively.
Fourth, in case of plastic flow, after having computed the return mapping, the updated stress tensor at time t_{n+1} is computed from Eq. (41). The internal variable η_i at time t_{n+1} are also obtained from this return mapping as well as the isotropic incremental-secant operator is obtained from either Eq. (58) or Eq. (64), for the residual- and zero-incremental-secant formulations, respectively.
Fifth, the "consistent" operators are obtained from (70) and (71).

(3) In order to solve the MFH iterations, Eq. (81) is rewritten as $\boldsymbol{F} = 0$, where $\boldsymbol{F}$ is the stress residual in the inclusion phase. During the time step $[t_n,\, t_{n+1}]$, the stress residual can be evaluated by considering $\Delta\bar{\boldsymbol{\varepsilon}}^{\mathrm{r}}_{n+1}$ constant, leading to [27, 50]

$$\begin{aligned}\boldsymbol{F} = \hat{\mathbb{C}}^{\mathrm{S}}_{0\,n+1} : \left[\Delta\bar{\boldsymbol{\varepsilon}}^{\mathrm{r}}_{\mathrm{I}\,n+1} - \frac{1}{v_0}\mathbb{S}^{-1} : (\,\Delta\bar{\boldsymbol{\varepsilon}}^{\mathrm{r}}_{\mathrm{I}\,n+1} - \Delta\bar{\boldsymbol{\varepsilon}}^{\mathrm{r}}_{n+1})\right] - \\ \hat{\mathbb{C}}^{\mathrm{S}}_{\mathrm{I}\;n+1} : \Delta\bar{\boldsymbol{\varepsilon}}^{\mathrm{r}}_{\mathrm{I}\,n+1} .\end{aligned} \tag{89}$$

(4) As long as the process did not converge, *i.e.* $|\boldsymbol{F}| > \mathrm{Tol}$, the strain increment in the inclusions phase is corrected following

$$\Delta\bar{\boldsymbol{\varepsilon}}^{\mathrm{r}}_{\mathrm{I}\,n+1} \leftarrow \Delta\bar{\boldsymbol{\varepsilon}}^{\mathrm{r}}_{\mathrm{I}\,n+1} - \mathbb{J}^{-1} : \boldsymbol{F} , \tag{90}$$

where the Jacobian matrix $\mathbb{J}$ is computed at constant $\Delta\bar{\boldsymbol{\varepsilon}}^{\mathrm{r}}_{n+1}$, such that $\delta\boldsymbol{F} = \mathbb{J} : \delta\bar{\boldsymbol{\varepsilon}}_{\mathrm{I}}$. As the Eshelby tensor $\mathbb{S}(\mathrm{I},\, \hat{\mathbb{C}}^{\mathrm{S}}_{0\,n+1})$ is not constant during this M-T process, its derivative with respect to $\Delta\bar{\boldsymbol{\varepsilon}}^{\mathrm{r}}_{0\,n+1}$ needs to be considered

too, leading to

$$\begin{aligned}\mathbb{J} &= \frac{\partial \boldsymbol{F}}{\partial \bar{\boldsymbol{\varepsilon}}_{\mathrm{I}}} + \frac{\partial \boldsymbol{F}}{\partial \bar{\boldsymbol{\varepsilon}}_{0}} : \left.\frac{\partial \bar{\boldsymbol{\varepsilon}}_{0}}{\partial \bar{\boldsymbol{\varepsilon}}_{\mathrm{I}}}\right|_{\Delta \bar{\boldsymbol{\varepsilon}}^{\mathrm{r}}_{n+1}} = \frac{\partial \boldsymbol{F}}{\partial \bar{\boldsymbol{\varepsilon}}_{\mathrm{I}}} - \frac{v_{\mathrm{I}}}{v_0}\frac{\partial \boldsymbol{F}}{\partial \bar{\boldsymbol{\varepsilon}}_{0}} \\ &= \hat{\mathbb{C}}^{\mathrm{S}}_{0\,n+1} : \left[\mathbb{I} - \mathbb{S}^{-1}\right] - \hat{\mathbb{C}}^{\mathrm{S}}_{\mathrm{I}\,n+1} - \frac{\partial\, \hat{\mathbb{C}}^{\mathrm{S}}_{\mathrm{I}\,n+1}}{\partial \boldsymbol{\varepsilon}_{\mathrm{I}}} : \Delta \bar{\boldsymbol{\varepsilon}}^{\mathrm{r}}_{\mathrm{I}\,n+1} - \\ &\quad \frac{v_{\mathrm{I}}}{v_0}\frac{\partial\, \hat{\mathbb{C}}^{\mathrm{S}}_{0\,n+1}}{\partial \bar{\boldsymbol{\varepsilon}}_{0}} : \left[\Delta \bar{\boldsymbol{\varepsilon}}^{\mathrm{r}}_{\mathrm{I}\,n+1} - \mathbb{S}^{-1} : \frac{\left(\Delta \bar{\boldsymbol{\varepsilon}}^{\mathrm{r}}_{\mathrm{I}\,n+1} - \Delta \bar{\boldsymbol{\varepsilon}}^{\mathrm{r}}_{n+1}\right)}{v_0}\right] - \\ &\quad \frac{v_{\mathrm{I}}}{v_0}\, \hat{\mathbb{C}}^{\mathrm{S}}_{0\,n+1} : \mathbb{S}^{-1} - \\ &\quad \frac{v_{\mathrm{I}}}{v_0^2}\, \hat{\mathbb{C}}^{\mathrm{S}}_{0\,n+1} \otimes \left(\Delta \bar{\boldsymbol{\varepsilon}}^{\mathrm{r}}_{\mathrm{I}\,n+1} - \Delta \bar{\boldsymbol{\varepsilon}}^{\mathrm{r}}_{n+1}\right) :: \left(\mathbb{S}^{-1} \otimes \mathbb{S}^{-1}\right) :: \frac{\partial \mathbb{S}}{\partial \bar{\boldsymbol{\varepsilon}}_{0}}\,, \end{aligned} \tag{91}$$

where $\frac{\partial \hat{\mathbb{C}}^{\mathrm{S}}_{i\ n+1}}{\partial \bar{\boldsymbol{\varepsilon}}_{i}}$ are given in A.1, and where $\frac{\partial \mathbb{S}}{\partial \bar{\boldsymbol{\varepsilon}}_{0}}$ is given in Appendix A.3.

(5) A new iteration can then be performed.

- After convergence, the time step is finalised by evaluating
  (1) The homogenised stress from Eq. (80)

$$\bar{\boldsymbol{\sigma}}_{n+1} = v_0\, \bar{\boldsymbol{\sigma}}_{0\,n+1} + v_{\mathrm{I}}\, \bar{\boldsymbol{\sigma}}_{\mathrm{I}\,n+1}\ , \tag{92}$$

and the updated strain tensors

$$\begin{aligned} \bar{\boldsymbol{\varepsilon}}_{n+1} &= \bar{\boldsymbol{\varepsilon}}^{\mathrm{res}}_{n} + \Delta \bar{\boldsymbol{\varepsilon}}^{\mathrm{r}}_{n+1} \\ \bar{\boldsymbol{\varepsilon}}_{\mathrm{I}\,n+1} &= \bar{\boldsymbol{\varepsilon}}^{\mathrm{res}}_{\mathrm{I}\ n} + \Delta \bar{\boldsymbol{\varepsilon}}^{\mathrm{r}}_{\mathrm{I}\,n+1} \\ \bar{\boldsymbol{\varepsilon}}_{0\,n+1} &= \bar{\boldsymbol{\varepsilon}}^{\mathrm{res}}_{0\ n} + \Delta \bar{\boldsymbol{\varepsilon}}^{\mathrm{r}}_{0\,n+1} \end{aligned} \tag{93}$$

  (2) The linearisation of the homogenised stress (80), which yields the "consistent" composite material operator (85). This result is completed by recalling that since $\boldsymbol{F} = 0$, the effect on the strain increment in each phase of a variation $\delta\Delta\bar{\boldsymbol{\varepsilon}}$ can directly be obtained by constraining $\delta \boldsymbol{F} = 0$, and one thus has

$$0 = \frac{\partial \boldsymbol{F}}{\partial \bar{\boldsymbol{\varepsilon}}_{\mathrm{I}}} : \delta\Delta \bar{\boldsymbol{\varepsilon}}^{\mathrm{r}}_{\mathrm{I}} + \frac{\partial \boldsymbol{F}}{\partial \bar{\boldsymbol{\varepsilon}}_{0}} : \delta\Delta \bar{\boldsymbol{\varepsilon}}^{\mathrm{r}}_{0} + \frac{\partial \boldsymbol{F}}{\partial \bar{\boldsymbol{\varepsilon}}} : \delta\Delta \bar{\boldsymbol{\varepsilon}}^{\mathrm{r}}\,. \tag{94}$$

This last equation and Eq. (79) yield directly

$$\frac{\partial \bar{\boldsymbol{\varepsilon}}_{\mathrm{I}}}{\partial \bar{\boldsymbol{\varepsilon}}} = -\mathbb{J}^{-1} : \frac{\partial \boldsymbol{F}}{\partial \bar{\boldsymbol{\varepsilon}}}\,, \text{ and} \tag{95}$$

$$\frac{\partial \bar{\boldsymbol{\varepsilon}}_{0}}{\partial \bar{\boldsymbol{\varepsilon}}} = \frac{1}{v_0}\left(\mathbb{I} - v_{\mathrm{I}}\frac{\partial \bar{\boldsymbol{\varepsilon}}_{\mathrm{I}}}{\partial \bar{\boldsymbol{\varepsilon}}}\right)\,. \tag{96}$$

The expression of the missing term $\frac{\partial \boldsymbol{F}}{\partial \bar{\boldsymbol{\varepsilon}}}$ is detailed in Appendix A.4.

5. Numerical simulations

In this section the predictions of the developed incremental-secant MFH accounting for the second statistical moment estimation of the von Mises stress are studied.

First the two formulations, *i.e.* the residual- and zero-incremental-secant methods, are compared for composite materials with short and long elastic fibres. This new MFH with second statistical moment estimations is then applied on several composite material systems, for different triaxiality and loading conditions, and the predictions are compared to other MFH schemes with first or second statistical moment estimations.

For all the simulations, the predictions have converged with the strain increment size.

5.1. *Comparison of the residual- and zero-incremental-secant assumptions*

First we compare the results obtained with the second statistical moments estimations with

- the residual-incremental-secant method and with the full second statistical moment estimation of the von Mises stress (53) –denoted "2nd-mom. res.-incr.-sec." in the figures;
- the zero-incremental-secant method and with the second statistical moment estimation of the von Mises stress (68) –denoted "2nd-mom. 0-incr.-sec." in the figures.
- These predictions are also compared to the ones obtained with the residual- or zero-incremental-secant with first statistical moment estimation of the von Mises stress [27] –denoted "1st-mom. res.-incr.-sec." or "1st-mom. 0-incr.-sec." in the figures.

We consider the cases of an elasto-plastic matrix reinforced with short and long elastic fibres, as these two cases lead to high contrast in the matrix von Mises stress, usually responsible for poor MFH predictions, but also the case of inclusions having a lower plastic hardening than the matrix material.

5.1.1. Short glass fibre reinforced polyamide (GFRP)

Aligned short glass fibres, with a volume fraction $v_{\rm I} = 15.7\%$ and an aspect ratio $\alpha = 15$, reinforce a polyamide matrix. The elasto-plastic material of the matrix obeys to an exponential-linear hardening law:

$$R(p) = k_1 p + k_2(1 - e^{-mp})\,. \tag{97}$$

The material properties are

- Inclusions: $E_{\rm I} = 72$GPa, $\nu_{\rm I} = 0.22$;
- Matrix: $E_0 = 2.1$GPa, $\nu_0 = 0.3$, $\sigma_{Y0} = 29$MPa, $k_{10} = 139.0$MPa, $k_{20} = 32.7$MPa and $m_0 = 319.4$.

The finite element (FE) simulations [41] are used as a reference.

Fig. 3 compares the different predictions for a loading in the fibres direction. The residual-incremental-secant method with the second statistical moment estimation of the von Mises stress over-estimates the composite homogenised stress as it can be seen in 3(a). As illustrated in Fig. 3(a), the zero-incremental-secant MFH with second statistical moment estimations yields better predictions of the homogenised composite material, although plastic yielding still occurs later than in the FE results. The evolution of the average stress in the inclusion phase is reported in Fig. 3(b), where it can be seen that only the zero-incremental-secant method with second statistical moment estimations is close to the FE results. This is explained by the higher value reached by the second statistical moment estimation of the yield stress predicted in the matrix phase, see Fig. 3(c). Note that the second statistical

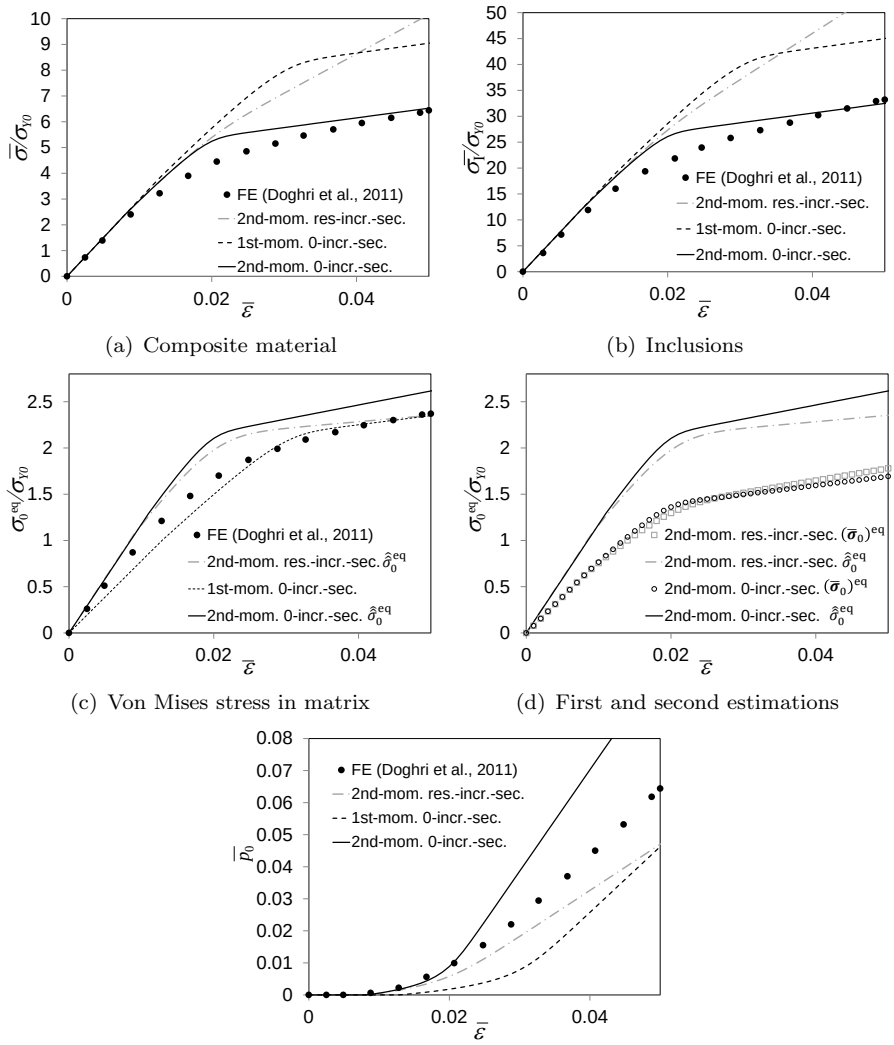

(a) Composite material (b) Inclusions

(c) Von Mises stress in matrix (d) First and second estimations

(e) Plastic strain in matrix

Figure 3. Comparison of the approximations predictions for the short glass fibre reinforced polyamide test loaded in the longitudinal direction: (a) Mean composite material stress along the loading direction; (b) Mean inclusions phase stress in the loading direction; (c) Von Mises stress in the matrix phase (d) First (markers) and second (lines) statistical estimations of the von Mises stress in the matrix phase; and (e) Mean accumulated plastic strain in the matrix phase.

moment estimations of the incremental-secant method are always higher than the average value as illustrated in Fig. 3(d). However, the zero-incremental-secant MFH with second statistical moment estimations is accompanied by a over-prediction of the accumulated plastic strain, see Fig. 3(e).

Overall the zero-incremental-secant MFH with second statistical moment estimation of the von Mises stress predicts results closer to the FE solution than the predictions obtained with the first statistical moment estimation of the von Mises stress.

5.1.2. Aluminum alloy matrix reinforced with continuous stiff alumina fibres

Continuous alumina fibres, with a volume fraction of $v_{\mathrm{I}} = 55\%$, reinforce an aluminum alloy matrix. The hardening law of the matrix reads

$$R(p) = kp^m\,, \tag{98}$$

where k and m are the hardening parameters. The Metal Matrix Composite (MMC) material is characterised by the phase properties: [51]

- Inclusions: $E_{\mathrm{I}} = 344.5\mathrm{GPa}$, $\nu_{\mathrm{I}} = 0.26$;
- Matrix: $E_0 = 68.9\mathrm{GPa}$, $\nu_0 = 0.32$, $\sigma_{Y0} = 94\mathrm{MPa}$, $k_0 = 578.25\mathrm{MPa}$ and $m_0 = 0.529$.

The FE predictions reported in [52] are used as a reference solution.

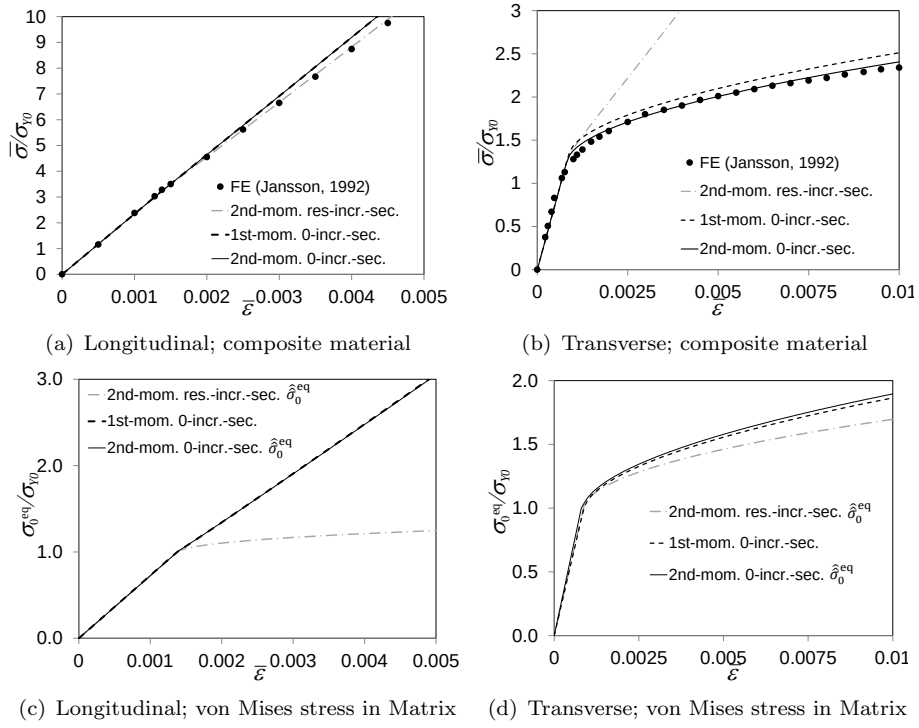

(a) Longitudinal; composite material

(b) Transverse; composite material

(c) Longitudinal; von Mises stress in Matrix

(d) Transverse; von Mises stress in Matrix

Figure 4. Comparison of the approximations predictions for continuous stiff alumina fibres reinforced aluminum alloy matrix test loaded in the (a & c) longitudinal direction and in the (b & d) transverse direction. (a & b) Mean composite material stress along the loading direction; (c & d) Von Mises stress in the matrix phase.

The predictions for the different assumptions are illustrated in Fig. 4 and lead to the same conclusions as for the GFRP test. The residual-incremental-secant MFH with the second statistical moment estimation of the von Mises stress over-predicts the results in the transverse direction, see Fig. 4(b), while the zero-incremental formulations with first and second statistical moment estimations of the von Mises stress yield the correct behaviours.

5.1.3. MMC with low inclusions phase hardening

Up to now the examples considered elastic inclusions embedded in an elasto-plastic matrix, in which case the 0-incremental-secant method should be used in the matrix phase. However when developing the incremental-secant method [27], it was shown that if the inclusions phase is characterised by a low-hardening elasto-plastic response, the residual method should be considered in both phases (in both cases the inclusions phase should consider the residual-incremental-secant method). In this subsection we intend to show that this behaviour is still true with the second statistical moment estimations.

To this end we consider a composite material made of elasto-plastic spherical austenite inclusions embedded in an elasto-plastic ferrite matrix [51]. In this case, the inclusions are more compliant than the matrix, see Fig. 5(a). The inclusion and matrix hardening laws follow Eq. (98), with the parameters

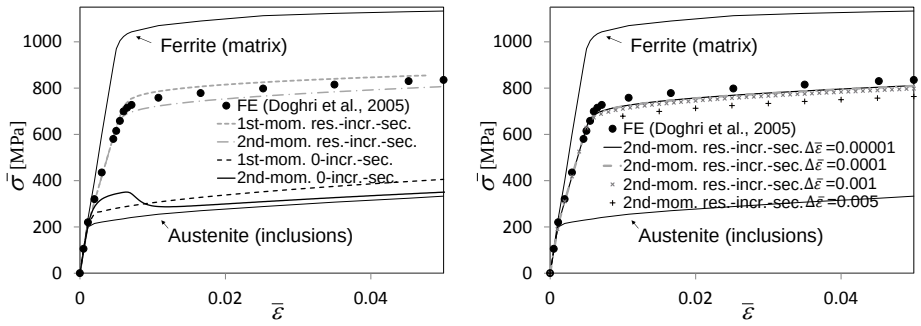

(a) Scheme effect (b) $\Delta\bar{\varepsilon}$ effect

Figure 5. Results for MMC with low-hardening elasto-plastic inclusions embedded in a higher-hardening elasto-plastic matrix. (a) Effect of the residual method, (b) Effect of the strain increment $\Delta\bar{\varepsilon}$ size.

- Inclusions: $E_{\mathrm{I}} = 179.35$GPa, $\nu_{\mathrm{I}} = 0.3$, $\sigma_{Y\mathrm{I}} = 202$MPa, $k_{\mathrm{I}} = 688$MPa and $m_{\mathrm{I}} = 0.55$;
- Matrix: $E_0 = 196.85$GPa, $\nu_0 = 0.3$, $\sigma_{Y0} = 600$MPa, $k_0 = 650$MPa and $m_0 = 0.06$.

The inclusions volume fraction is $v_{\mathrm{I}} = 35\%$.

The predictions of the incremental-secant MFH scheme with both the first and second statistical moment estimations are reported in Fig. 5(a). Good estimations are obtained with the residual-incremental-secant MFH, although the composite response is slightly overestimated with the first statistical moment method and under-estimated with the second statistical moment scheme. Note that the 0-incremental-secant MFH with second statistical moment estimations predicts a spurious softening. This is explained by the use of the approximation (67) in the matrix phase, in place of the full expression (35).

The effect of the strain increment $\Delta\bar{\varepsilon}$ size on the prediction is reported in Fig. 5(b), where it can be seen that the solution converges when decreasing this increment size. Practically 50 increments are enough to reach the convergence.

5.1.4. MMC with elasto-perfectly-plastic phases

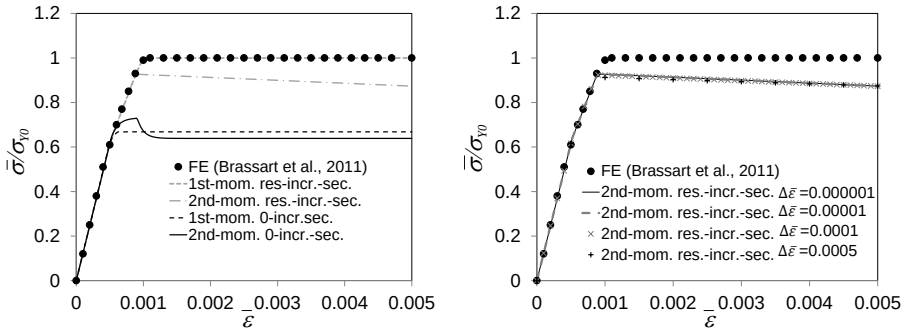

(a) Scheme effect (b) $\Delta\bar{\varepsilon}$ effect

Figure 6. Results for composites with elasto-perfectly-plastic inclusions with a low hardening embedded in an elasto–plastic matrix. (a) Effect of the residual method, (b) Effect of the strain increment $\Delta\bar{\varepsilon}$ size.

The effect of the residual is eventually studied on a composite material where both phases, matrix and inclusions, are elastic-perfectly-plastic ($R_{\mathrm{I}}(p) = R_0(p) = 0$). The other material properties are

- Inclusions: $E_{\mathrm{I}} = 400$GPa, $\nu_{\mathrm{I}} = 0.2$, $\sigma_{Y\mathrm{I}} = 75$MPa;
- Matrix: $E_0 = 75$GPa, $\nu_0 = 0.3$, $\sigma_{Y0} = 75$MPa.

The volume fraction of the spherical inclusions is $v_I = 15\%$. The FE estimations reported in [45] are used as a reference solution.

As it can be seen in Fig. 6(a) the residual in the matrix phase has to be considered for the first and second statistical moment estimations in order to capture the correct behaviour. One more time, the 0-incremental-secant MFH with second statistical moment estimations predicts a spurious softening due to the approximation (67). However, in this case, the residual-incremental-secant MFH with the second statistical moment estimation of the von Mises stress leads also to a softening of the composite. This can be explained as this estimation is higher than the first moment estimation as it will be discussed in details in Section 6, although for an elastic-perfectly-plastic material the two values should eventually converge. This is a limitation of the second statistical moment estimation. Such a limitation was already seen with the variational method developed in [45], for which the predictions are too compliant and depend on the strain increment size. With the residual-incremental-secant method the results are found to be independent of the strain increment, see Fig. 6(b).

5.2. *Comparison of the 0-incremental-secant MFH with second statistical moment estimations with other MFH schemes*

In this section, the predictions obtained with the zero-incremental-secant MFH with a second statistical moment estimation of the von Mises stress are compared on various composite materials with the predictions obtained with other MFH schemes, in particular with

- the incremental-tangent MFH with first statistical moment estimations [16, 18];
- the incremental-tangent MFH with second statistical moment estimations [41];
- the zero-incremental-secant MFH with first statistical moment estimations [27];
- the incremental variational formulations [45–47].

5.2.1. Short glass fibre reinforced polyamide (GFRP)

The material system is the same as in 5.1.1, but this time we compare the results obtained by various MFH schemes for loading in the longitudinal and transverse directions.

For this test, the predictions obtained with the first and second statistical moment estimations for both the incremental-secant and the incremental-tangent MFH scheme are compared with the FE results [41], which are used as a reference. It can be seen in Fig. 7 that for a transverse loading, all the methods predict similar results. However for a longitudinal loading the MFH scheme with first statistical moment estimations of the von Mises stress over-predicts the composite material response, see Fig. 7(a). The homogenisation methods accounting for the second statistical moment estimations of the von Mises stress are more accurate. In particular the new incremental-secant method predicts a composite material response closer to the FE results than the incremental-tangent method, see Fig. 7(a). This is due to the evolution of the plastic strain in the matrix phase which is overestimated with the new incremental-secant method, while it is under-estimated with the incremental-tangent method, see Fig. 7(e).

We are now considering the same material system but with the matrix phase having a value of the Young modulus E_0 divided by two. As a result it is expected for the composite material to be softer during the elastic response, but also during the elasto-plastic response. Both first and second statistical moment estimations lead to this result for a transverse loading as it can be seen in Fig. 8(b). However for the longitudinal loading, see Fig. 8(a), it appears that only the incremental-

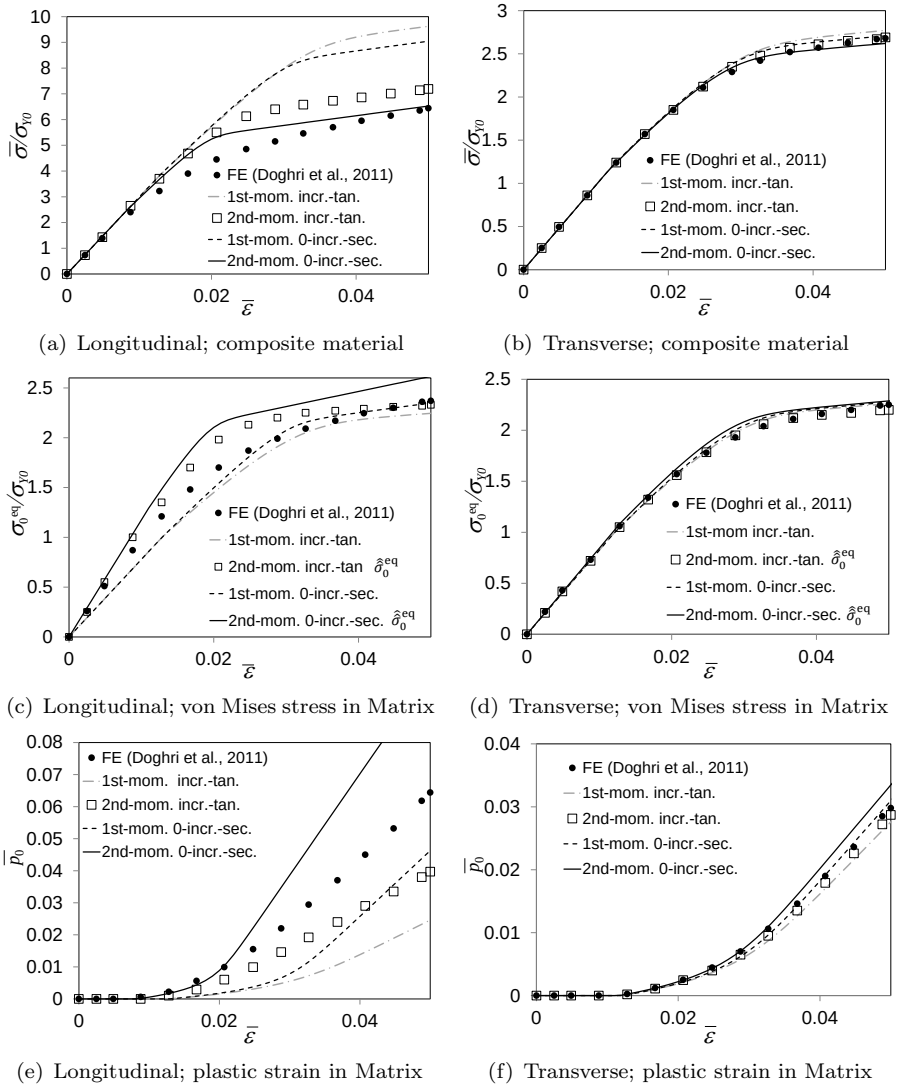

(a) Longitudinal; composite material

(b) Transverse; composite material

(c) Longitudinal; von Mises stress in Matrix

(d) Transverse; von Mises stress in Matrix

(e) Longitudinal; plastic strain in Matrix

(f) Transverse; plastic strain in Matrix

Figure 7. Comparison of the different MFH schemes predictions for the short glass fibre reinforced polyamide test loaded in (left column) the longitudinal direction and in (right column) the transverse direction: (a & b) Mean composite material stress along the loading direction; (c & d) Von Mises stress in the matrix phase; and (e & f) Mean accumulated plastic strain in the matrix phase.

secant method with second statistical moment estimations of the von Mises stress leads to consistent results. With a first statistical moment estimation of the von Mises stress, the composite material response, see Fig. 8(a), and the fibres phase response, see Fig. 8(c), reach a higher level in the case of a lower matrix Young modulus. This is due to the increasing delay in the predicted plastic yield point resulting from a first statistical moment estimation.

5.2.2. Triaxiality effect

The reliability of the developed zero-incremental-secant MFH scheme with second statistical moment estimations is now ascertained under different triaxiality states defined by $T = \mathrm{tr}(\bar{\boldsymbol{\sigma}})/3\bar{\sigma}^{eq}$: pure shearing, biaxial loading, and a plane strain tension/compression loading.

- The shear loading is characterised by $\bar{\sigma}_{12} = \bar{\sigma}_{21} = \sigma$ with the other components of the stress tensor $\bar{\boldsymbol{\sigma}}$ being zero. This corresponds to a triaxiality ratio of 0.
- The biaxial loading is characterised by $\bar{\sigma}_{11} = \bar{\sigma}_{22} = \sigma$ and $\bar{\sigma}_{33} = 0$. The corresponding triaxiality ratio is 2/3.

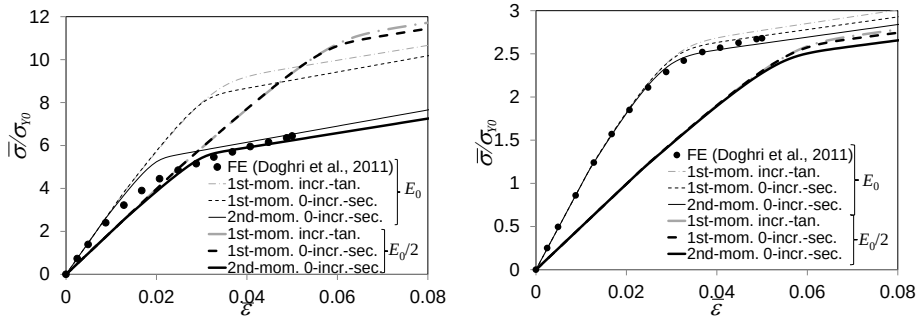

(a) Longitudinal; composite material (b) Transverse; composite material

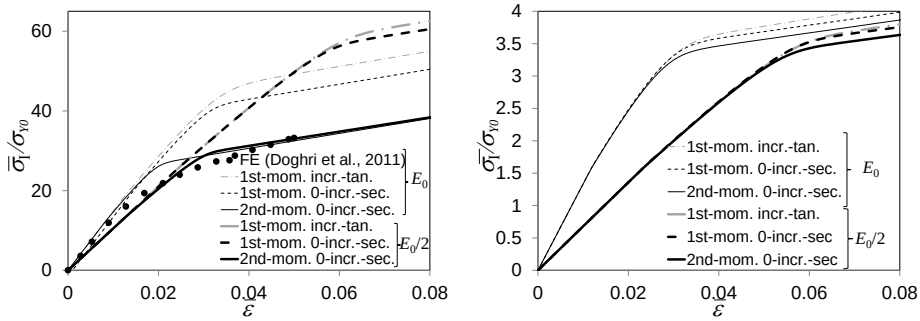

(c) Longitudinal; inclusions (d) Transverse; inclusions

Figure 8. Comparison of the different MFH schemes predictions for the short glass fibre reinforced polyamide test loaded in (left column) the longitudinal direction and in (right column) the transverse direction. The thin lines are related to the original material system and the thick lines to the material system with the matrix phase having a lower Young modulus. (a & b) Mean composite material stress along the loading direction; (c & d) Mean inclusions phase stress along the loading direction.

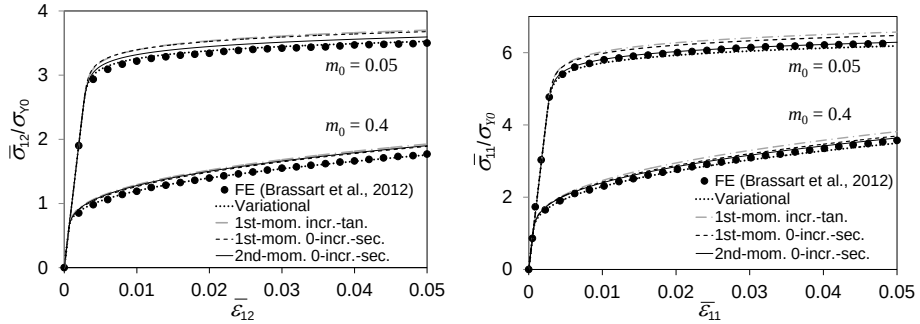

(a) Pure shearing

(b) Biaxial tension

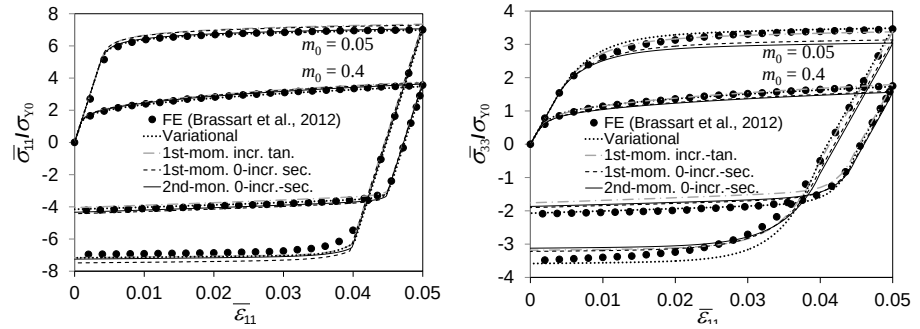

(c) Tension-compression, 11-loading stress

(d) Tension-compression, 33-reaction stress

Figure 9. Results for SiC-particles reinforced aluminum matrix under different triaxiality states. The first statistical moment solutions are from [27].

- For the case of plane strain tension/compression, the only non–zero components of $\bar{\boldsymbol{\varepsilon}}$ are $\bar{\varepsilon}_{11}$ and $\bar{\varepsilon}_{22}$, where $\bar{\varepsilon}_{22}$ is computed to satisfy $\bar{\sigma}_{22} = 0$. This results in a

triaxiality ratio of approximately 1 during the plastic flow.

The considered composite material is a SiC-particles reinforced aluminum matrix. The elasto-plastic metal matrix follows the power-law hardening (98) and the material properties are

- Inclusions: $E_{\mathrm{I}} = 400\mathrm{GPa}$, $\nu_{\mathrm{I}} = 0.2$;
- Matrix: $E_0 = 75\mathrm{GPa}$, $\nu_0 = 0.3$, $\sigma_{Y0} = 75\mathrm{MPa}$, $k_0 = 400\mathrm{MPa}$ and $m_0 = 0.4$ or $m_0 = 0.05$.

The volume fraction of the spherical inclusions is $v_{\mathrm{I}} = 15\%$. The finite element predictions available in [46] are used as reference solutions.

The predictions of the 0-incremental-secant formulation with a second statistical moment estimation of the von Mises stress are presented in Fig. 9 and are compared to the results obtained using first statistical moment estimations and using a variational homogenisation scheme [46]. The new scheme is accurate for all the triaxiality conditions and is shown to slightly improve the prediction as compared to the MFH using first statistical moment estimation, in particular for $m_0 = 0.05$, see Figs. 9(a) and 9(b).

5.2.3. Non-monotonic and non-proportional loading path

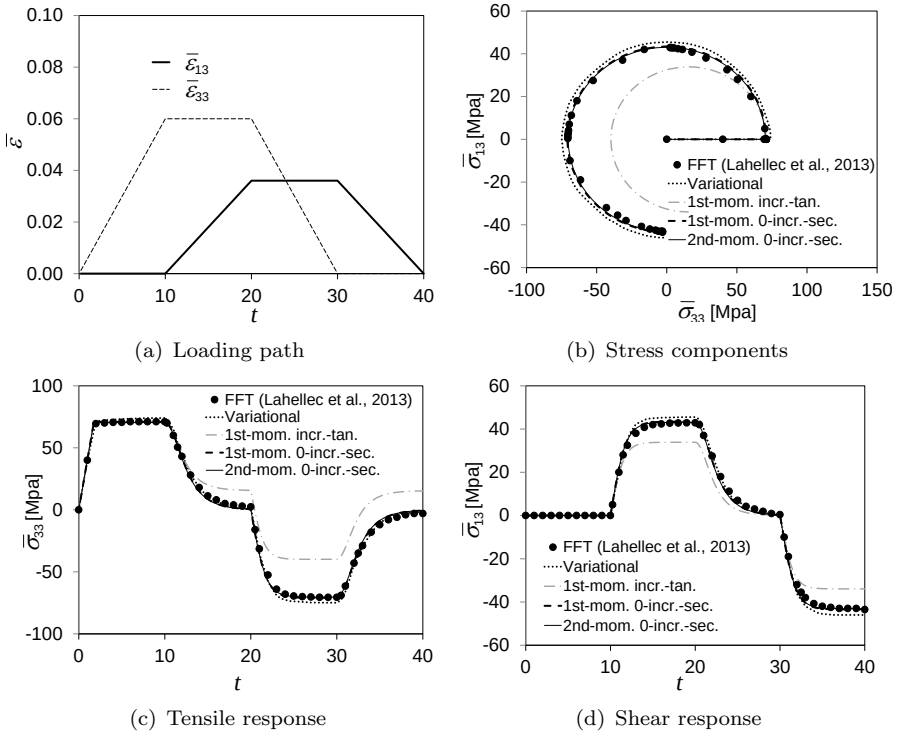

(a) Loading path (b) Stress components

(c) Tensile response (d) Shear response

Figure 10. Results for a non–monotonic and non–proportional loading path. (a) Applied strain components history, (b) comparisons of the predicted stress components, (c and d) comparison of the predicted stress components history. The first statistical moment solutions are from [27].

One of the main advantages of the incremental-secant MFH method is its ability to handle non-monotonic and non-proportional loadings, as it has been shown with first statistical moment estimations [27]. There is theoretically no reason to loose this ability when considering the second statistical moment estimations, but this is actually demonstrated in this section by considering the example proposed in [47], in which the external boundary conditions correspond to constraining simultane-

ously all the strain components following

$$\bar{\boldsymbol{\varepsilon}}(t) = \bar{\varepsilon}_{33}(t)\left[\boldsymbol{e}_3 \otimes \boldsymbol{e}_3 - \frac{1}{2}(\boldsymbol{e}_1 \otimes \boldsymbol{e}_1 + \boldsymbol{e}_2 \otimes \boldsymbol{e}_2)\right] + \bar{\varepsilon}_{13}(t)(\boldsymbol{e}_1 \otimes \boldsymbol{e}_3 + \boldsymbol{e}_3 \otimes \boldsymbol{e}_1 + \boldsymbol{e}_2 \otimes \boldsymbol{e}_3 + \boldsymbol{e}_3 \otimes \boldsymbol{e}_2)\ . \quad (99)$$

The evolutions of the two strains are illustrated in Fig. 10(a), leading to a the non–monotonic and non–proportional loading,

The material system consists of elastic spherical inclusions, with a volume fraction of $v_{\mathrm{I}} = 17\%$, embedded in an elasto-perfectly-plastic matrix, with the following material properties

- Inclusions: $\kappa_{\mathrm{I}}^{\mathrm{el}} = 20\mathrm{GPa}$, $\mu_{\mathrm{I}}^{\mathrm{el}} = 6\mathrm{GPa}$;
- Matrix: $\kappa_0^{\mathrm{el}} = 10\mathrm{GPa}$, $\mu_0^{\mathrm{el}} = 3\mathrm{GPa}$, $\sigma_{Y0} = 100\mathrm{MPa}$.

This reference solution was obtained with a Fast Fourier Transforms (FFT)-based homogenisation method in [47].

The predictions of the 0-incremental-secant MFH with a second statistical moment estimation of the von Mises stress are presented in Fig. 10 and are compared to the results obtained using first statistical moment estimations and using a variational MFH scheme [47]. It can be seen that the 0-incremental-secant MFH prediction with the first or second statistical moment estimations nearly coincide with the FE predictions, while the incremental-tangent method is unable to handle the non-proportional loading.

6. Discussion

In the proposed MFH process, the Mori-Tanaka scheme is applied to homogenise the linear comparison composite (LCC). Some remarks can be made:

- The method can be easily implemented by using the constitutive material boxes of an existing material library as the MFH scheme directly calls these material laws, as shown in Section 4.
- According to the Mori-Tanaka scheme, there is no stress fluctuation in the inclusions. Therefore, in the incremental formulation, increments of stress in the inclusions phase are always uniform, and the second statistical moment estimation of the von Mises stress of the inclusions equals to the von Mises stress calculated from the first statistical moment average [47].
- During the elasto-plastic stage of the composite material deformation process, a part of one phase exhibits plastic flow while the other part remains elastic. There is thus an important difference in the local material operators within one phase, which reduces the accuracy of a homogenisation method based on the mean-field values.
- Compared to an incremental-tangent method, the incremental-secant method exhibits less fluctuation in the local material operators within the composite material phases as these operators are evaluated from an unloaded virtual state and not from the previous stress state. The slope of the operator is thus less decreased during the plastic flow. The incremental-secant MFH method exhibits more accurate predictions than the incremental-tangent method, as shown in [27] for first statistical moment estimations [27] and in Section 5 for second statistical moment estimations predictions.
- The fluctuation in the local material operators is particularly important in the case of short fibres for which a plastic zone develops in the matrix first at both

ends of the fibres in the case of a longitudinal loading [41]. Because of this plastic-flow the inclusion loading is lower than in the elastic case. The composite behaviour can thus only be predicted if the plastic yield is correctly captured. The incremental-secant MFH with first statistical moment estimations is not able to capture this plastic yield with a good accuracy. We have show in Section 5 that the incremental-secant MFH with second statistical moment estimations leads to better predictions of the composite material and phases responses since the second statistical estimation of the von Mises stress reach the material yield stress in the matrix sooner than its first statistical estimation, leading to a more important plastic flow in the average sense.

- In the matrix phase, the equation for the second statistical moment of the equivalent trial stress increment (5) reads

$$\begin{aligned}\Delta\hat{\bar{\sigma}}_0^{\mathrm{tr}\,\mathrm{eq}} &= 3\mu_0^{\mathrm{el}}\sqrt{\frac{2}{3}\mathbb{I}^{\mathrm{dev}} :: \langle \Delta\boldsymbol{\varepsilon}^{\mathrm{r}} \otimes \Delta\boldsymbol{\varepsilon}^{\mathrm{r}}\rangle_{\omega_0}} \\ &= 3\mu_0^{\mathrm{el}}\sqrt{\frac{2}{3v_0}\mathbb{I}^{\mathrm{dev}} :: \Delta\bar{\boldsymbol{\varepsilon}}^{\mathrm{r}} : \frac{\partial\bar{\mathbb{C}}^{\mathrm{el}}}{\partial\mathbb{C}_0^{\mathrm{el}}} : \Delta\bar{\boldsymbol{\varepsilon}}^{\mathrm{r}}}\,. \end{aligned} \tag{100}$$

As a consequence, the evaluation of the second statistical-estimation of the von Mises stress does not depend only on the average stress tensor, but also on the material operator. The second statistical moment estimation of the von Mises stress remains higher than its first statistical moment estimation. Indeed, defining $\delta\Delta\boldsymbol{\sigma}(\boldsymbol{x})$ as the fluctuation around the mean value $\Delta\bar{\boldsymbol{\sigma}}$, one has in the matrix phase

$$\begin{aligned}\left(\Delta\hat{\bar{\sigma}}_0^{\mathrm{eq}}\right)^2 &= \frac{3}{2}\left\langle (\Delta\bar{\boldsymbol{\sigma}} + \delta\Delta\boldsymbol{\sigma}(\boldsymbol{x})) : \mathbb{I}^{\mathrm{dev}} : (\Delta\bar{\boldsymbol{\sigma}} + \delta\Delta\boldsymbol{\sigma}(\boldsymbol{x}))\right\rangle_{\omega_0} \\ &= \frac{3}{2}\left\langle \Delta\bar{\boldsymbol{\sigma}} : \mathbb{I}^{\mathrm{dev}} : \Delta\bar{\boldsymbol{\sigma}}\right\rangle_{\omega_0} + 3\left\langle \Delta\bar{\boldsymbol{\sigma}} : \mathbb{I}^{\mathrm{dev}} : \delta\Delta\boldsymbol{\sigma}(\boldsymbol{x})\right\rangle_{\omega_0} + \\ &\quad \frac{3}{2}\left\langle \delta\Delta\boldsymbol{\sigma}(\boldsymbol{x}) : \mathbb{I}^{\mathrm{dev}} : \delta\Delta\boldsymbol{\sigma}(\boldsymbol{x})\right\rangle_{\omega_0} = \Delta\bar{\sigma}_0^{\mathrm{eq}} + \left(\delta\Delta\hat{\bar{\sigma}}_0^{\mathrm{eq}}\right)^2\,. \end{aligned} \tag{101}$$

The limitation of this method arises for elasto-perfectly-plastic material. Indeed in such a case at some point the local stress becomes uniform in the phase. Hence the first and second statistical moment estimations should be similar, which is not explicitly constrained in the proposed incremental-secant framework, yielding an apparent softening.

- From the descriptions above, we can say that the proposed second statistical moment method is more meaningful for the cases of a matrix reinforced with harder inclusions, as it was confirmed by the numerical simulations.

The development of the incremental-secant MFH with second statistical moment estimations paves the ways to two future developments.

- On the one hand, as shown in Section 5.2.1, the method allows capturing the change in the short fibre reinforced composite material response when the Young modulus of the matrix changes. This was not the case with the first statistical moment estimations. In the future we will take advantage of this accurate prediction to extend the method to visco-elastic and visco-plastic composite materials, for which a change in the phase stiffness with the strain rate should be consistently captured.
- On the other hand, as previously stated, the incremental-secant MFH formal-

ism was shown to be able to account for material softening when extended to include a non-local damage model in the matrix phase, thus enabling an accurate simulation of the onset and evolution of damage across the scales. Although the incremental-secant MFH method with second statistical estimations is not developed yet to account for damage, to illustrate the interest of the incremental-secant MFH method, we study the problem of continuous elastic isotropic fibres, with a volume fraction of $v_{\mathrm{I}} = 50\%$, embedded in a matrix material that follows a damage-enhanced elasto–plastic behavior. In order to avoid the loss of solution uniqueness caused by the matrix material softening, an implicit non-local formulation [32–35] of the matrix damage evolution is considered during the homogenization process. Details on this non-local damage-enhanced incremental-secant MFH formulation with first statistical moment estimations can be found in [29]. The composite material is loaded transversely under plane-stress state in the other transverse direction and plane-strain state in the longitudinal direction, before being unloaded until reaching a zero-strain state. The material parameters read:

- Inclusions: $E_{\mathrm{I}} = 238\mathrm{GPa}$, $\nu_{\mathrm{I}} = 0.26$.
- Matrix: $E_0 = 2.89\mathrm{GPa}$, $\nu_0 = 0.3$, $\sigma_{Y0} = 35\mathrm{MPa}$, $h_0 = 73\mathrm{MPa}$, $m_0 = 60$, $S_0 = 2\mathrm{MPa}$, $s = 0.5$ and $p_C = 0$,

which follows the hardening law

$$R(p) = h\left(1 - e^{-mp}\right) , \tag{102}$$

and the Lemaitre-Chaboche damage law

$$\Delta D\left(\boldsymbol{x}\right) = \begin{cases} 0, & \text{if } \tilde{p}\left(\boldsymbol{x}\right) \leqslant p_C \ ; \\ \left(\frac{\frac{1}{2}\boldsymbol{\varepsilon}^{\mathrm{el}}(\boldsymbol{x}):\mathbb{C}^{\mathrm{el}}:\boldsymbol{\varepsilon}^{\mathrm{el}}(\boldsymbol{x})}{S}\right)^{s} \Delta\tilde{p}\left(\boldsymbol{x}\right), & \text{if } \tilde{p}\left(\boldsymbol{x}\right) > p_C \, . \end{cases} \tag{103}$$

In this expression, p_C is a plastic threshold for the damage evolution, S and s are the material parameters, and $\frac{1}{2}\boldsymbol{\varepsilon}^{\mathrm{el}} : \mathbb{C}^{\mathrm{el}} : \boldsymbol{\varepsilon}^{\mathrm{el}}$ is the strain energy release rate. In the non-local implicit approach [32–35], the non-local accumulated plastic strain $\tilde{p}$ considered in (103) is computed from the implicit formulation

$$\tilde{p}\left(\boldsymbol{x}\right) - \boldsymbol{\nabla}\cdot\left(\boldsymbol{c}_{\mathrm{g}}\cdot\boldsymbol{\nabla}\tilde{p}\left(\boldsymbol{x}\right)\right) = p\left(\boldsymbol{x}\right) \quad \forall\boldsymbol{x}\in\omega_i \, , \tag{104}$$

where $\boldsymbol{c}_{\mathrm{g}}$ is the characteristic squared lengths tensor. The non-local equation (104) is practically solved by introducing a new degree of freedom $\tilde{p}$ in the finite element resolution. The finite element predictions were obtained in [28].

The predictions obtained by the incremental-secant MFH process, using the residual-incremental-secant operator for the inclusion phase and the zero-incremental-secant operator for the matrix phase [29] are compared to the prediction obtained by a incremental-tangent method [28] in Fig. 11. When analysing the composite material response, see Fig. 11(a), it appears that during the softening stage the incremental-secant MFH scheme is closer to the reference solution. This is explained by analysing the behaviour of the fibres, see Fig. 11(b) during the softening of the matrix phase.

Because of non-local formulation of the matrix phase damage evolution stated by Eqs. (103-104), the multi-scale numerical model does not lose the solution uniqueness upon strain-softening of the composite material, and the solution remains mesh-independent as demonstrated in [28, 29]. As a result, macro-scale composite laminates can be studied using the non-local damage-enhanced MFH

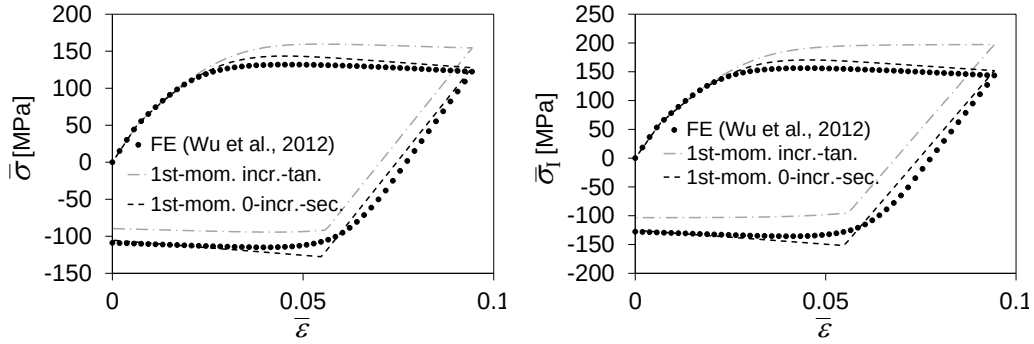

(a) Composite material (b) Inclusion phase

Figure 11. Comparison of the incremental-secant and incremental-tangent predictions for continuous-elastic fibres embedded in a matrix following a damage-enhanced elasto-plastic behavior. Figure adapted from [29]. (a) Average stress in the composite material along the loading direction. (b) Average stress in the inclusion phase along the loading direction.

and the strain localisation can be captured in the different plies [29, 53]. This is illustrated by considering a open-hole $[-45_2^o/45_2^o]_S$-laminate. Each ply is made of transverse-isotropic carbon-fibre-reinforced epoxy, with

- Inclusions: $E_{\mathrm{LI}} = 230\mathrm{GPa}$, $E_{\mathrm{TI}} = 40\mathrm{GPa}$, $\nu_{\mathrm{TTI}} = 0.2$, $\nu_{\mathrm{LTI}} = 0.256$, $G_{\mathrm{TTI}} = 16.7\mathrm{GPa}$, and $G_{\mathrm{LTI}} = 24\mathrm{GPa}$.
- Matrix: $E_0 = 3.2\mathrm{GPa}$, $\nu_0 = 0.3$, $\sigma_{Y0} = 15\mathrm{MPa}$, $h_0 = 300\mathrm{MPa}$, $m_0 = 100$, $S_0 = 0.1\mathrm{MPa}$, $s = 1.73$ and $p_C = 0$,

which follows the hardening law (102) and the damage law (103). The volume fraction of the continuous fibres is $v_{\mathrm{I}} = 60\%$.

Combining the non-local damage-enhanced incremental-secant MFH with a de-

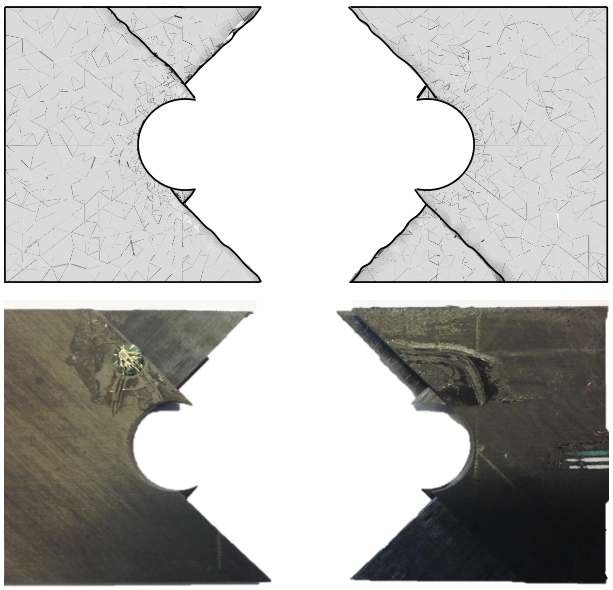

Figure 12. Delaminated parts of the $[45_2^o/-45_2^o]_S$-open hole sample for the (a) numerical model, (b) experimental sample. Figure adapted from [53].

lamination model as detailed in [53], allows modeling the failure of coupon tests. The configuration after total failure is illustrated for both the numerical (in which case damage reaches one) and experimental tests in Fig. 12. It can be seen on Fig. 12 that the damage bands of the numerical prediction are in good agreement with the crack initiation location in the different plies observed for

the experimental results, see Figure 12(b). This figure demonstrates the ability of the method to capture the failure mode of the test.

7. Conclusions

In this paper we have extended the incremental-secant MFH scheme to account for a second statistical moment estimation of the von Mises stress.

The method has the same advantages than the previously developed version with first statistical moment estimations, *i.e.* (i) the method can handle non-proportional and non-monotonic loading, (ii) the LCC operators used in the Eshelby tensor are naturally isotropic, avoiding the isotropisation approximation, (iii) the method can be easily implemented by using the constitutive material boxes of a material library as the MFH scheme directly calls these material laws, and (iv) a large variety of composite materials, at the exception of the elasto-perfectly-plastic inclusions case, can be modelled with this method in an accurate way.

When comparing the results obtained with the first and second statistical moment estimations, it appeared that the second statistical moment estimation improves the accuracy in the case of short fibres, while the prediction is of similar accuracy in the other cases.

Finally, it was shown that both formulations, *i.e.* with the first and second statistical moment estimations, require to cancel the residual stress in the matrix phase for composite materials whose inclusion phase remains elastic or has a plastic flow stiffer than its matrix phase.

In the future, it is intended to extend the incremental-secant MFH scheme with the second statistical moment estimations to visco-elastic, visco-plastic and to damage-enhanced elasto-plastic behaviours.

References

[1] P. Kanouté, D. Boso, J. Chaboche, and B. Schrefler, Archives of Computational Methods in Engineering 16 (2009), pp. 31–75, 10.1007/s11831-008-9028-8.
[2] M. Geers, V. Kouznetsova, and W. Brekelmans, Journal of Computational and Applied Mathematics 234 (2010), pp. 2175 – 2182.
[3] J.D. Eshelby, Proceedings of the Royal Society of London. Series A, Mathematical and Physical Sciences 241 (1957), pp. pp. 376–396.
[4] T. Mori and K. Tanaka, Acta Metallurgica 21 (1973), pp. 571–574, cited By (since 1996) 1814.
[5] Y. Benveniste, Mechanics of Materials 6 (1987), pp. 147 – 157.
[6] E. Kröner, Zeitschrift für Physik A Hadrons and Nuclei 151 (1958), pp. 504–518, 10.1007/BF01337948.
[7] R. Hill, Journal of the Mechanics and Physics of Solids 13 (1965), pp. 213 – 222.
[8] D.R.S. Talbot and J.R. Willis, IMA Journal of Applied Mathematics 35 (1985), pp. 39–54.
[9] D.R.S. Talbot and J.R. Willis, IMA Journal of Applied Mathematics 39 (1987), pp. 215–240.
[10] P. Ponte Castañeda, Journal of the Mechanics and Physics of Solids 39 (1991), pp. 45–71.
[11] P. Ponte Castañeda, SIAM Journal on Applied Mathematics 52 (1992), pp. 1321–1341.
[12] D. Talbot and J. Willis, International Journal of Solids and Structures 29 (1992), pp. 1981 – 1987.
[13] A. Molinari, F. El Houdaigui, and L. Tóth, International Journal of Plasticity 20 (2004), pp. 291 – 307.
[14] R. Hill, Journal of the Mechanics and Physics of Solids 13 (1965), pp. 89 – 101.
[15] H.E. Pettermann, A.F. Plankensteiner, H.J. Böhm, and F.G. Rammerstorfer, Computers & Structures 71 (1999), pp. 197 – 214.
[16] I. Doghri and A. Ouaar, International Journal of Solids and Structures 40 (2003), pp. 1681 – 1712.
[17] I. Doghri and L. Tinel, International Journal of Plasticity 21 (2005), pp. 1919 – 1940.

[18] O. Pierard and I. Doghri, International Journal for Multiscale Computational Engineering 4 (2006), pp. 521–543.
[19] A. Molinari, G. Canova, and S. Ahzi, Acta Metallurgica 35 (1987), pp. 2983–2994.
[20] R. Masson, M. Bornert, P. Suquet, and A. Zaoui, Journal of the Mechanics and Physics of Solids 48 (2000), pp. 1203 – 1227.
[21] A. Zaoui and R. Masson, *Modelling stress-dependent transformation strains of heterogeneous materials*, in *IUTAM Symposium on Transformation Problems in Composite and Active Materials*, Y.A. Bahei-El-Din, G.J. Dvorak, and G.M.L. Gladwell, eds., Solid Mechanics and Its Applications, Vol. 60, Springer Netherlands, 2002, pp. 3–15.
[22] O. Pierard and I. Doghri, International Journal of Plasticity 22 (2006), pp. 131 – 157.
[23] S. Mercier and A. Molinari, International Journal of Plasticity 25 (2009), pp. 1024 – 1048.
[24] I. Doghri, L. Adam, and N. Bilger, International Journal of Plasticity 26 (2010), pp. 219 – 238.
[25] J. Chaboche, P. Kanouté, and A. Roos, International Journal of Plasticity 21 (2005), pp. 1409 – 1434.
[26] M. Berveiller and A. Zaoui, Journal of the Mechanics and Physics of Solids 26 (1978), pp. 325 – 344.
[27] L. Wu, L. Noels, L. Adam, and I. Doghri, International Journal of Plasticity 51 (2013), pp. 80 – 102.
[28] L. Wu, L. Noels, L. Adam, and I. Doghri, Computer Methods in Applied Mechanics and Engineering 233-236 (2012), pp. 164–179.
[29] L. Wu, L. Noels, L. Adam, and I. Doghri, International Journal of Solids and Structures 50 (2013), pp. 3843 – 3860.
[30] J. Lemaitre and R. Desmorat, *Engineering damage mechanics: ductile, creep, fatigue and brittle failures*, Springer-Verlag, Berlin, 2005.
[31] J. Lemaitre, Computer Methods in Applied Mechanics and Engineering 51 (1985), pp. 31 – 49.
[32] R. Peerlings, R. de Borst, W. Brekelmans, and S. Ayyapureddi, Int. J. Numer. Meth. Engng 39 (1996), pp. 3391–3403.
[33] M. Geers, *Experimental analysis and computational modelling of damage and fracture*, Ph.D. thesis, University of Technology, Eindhoven (Netherlands)., 1997.
[34] R. Peerlings, R. de Borst, W. Brekelmans, and M. Geers, Mech. Cohesive-Frictional Mat. 3 (1998), pp. 323–342.
[35] R. Peerlings, M. Geers, R. de Borst, and W. Brekelmans, Int. J. Solids Structures 38 (2001), pp. 7723–7746.
[36] H. Moulinec and P. Suquet, European Journal of Mechanics - A/Solids 22 (2003), pp. 751 – 770.
[37] P. Ponte Castañeda, Journal of the Mechanics and Physics of Solids 44 (1996), pp. 827 – 862.
[38] P. Suquet, Comptes Rendus de l" Académie des Sciences 320 (1995), pp. 563–571.
[39] P. Ponte Castañeda, Journal of the Mechanics and Physics of Solids 50 (2002), pp. 737 – 757.
[40] P. Ponte Castañeda, Journal of the Mechanics and Physics of Solids 50 (2002), pp. 759 – 782.
[41] I. Doghri, L. Brassart, L. Adam, and J.S. Gérard, International Journal of Plasticity 27 (2011), pp. 352 – 371.
[42] N. Lahellec and P. Suquet, Journal of the Mechanics and Physics of Solids 55 (2007), pp. 1932 – 1963.
[43] N. Lahellec and P. Suquet, Journal of the Mechanics and Physics of Solids 55 (2007), pp. 1964 – 1992.
[44] N. Lahellec, P. Ponte Castañeda, and P. Suquet, Proceedings of the Royal Society A: Mathematical, Physical and Engineering Science 467 (2011), pp. 2224–2246.
[45] L. Brassart, L. Stainier, I. Doghri, and L. Delannay, Journal of the Mechanics and Physics of Solids 59 (2011), pp. 2455 – 2475.
[46] L. Brassart, L. Stainier, I. Doghri, and L. Delannay, International Journal of Plasticity 36 (2012), pp. 86 – 112.
[47] N. Lahellec and P. Suquet, International Journal of Plasticity (2013).
[48] M. Bobeth and G. G. Diener, Journal of the Mechanics and Physics of Solids 35 (1987), pp. 137 – 149.
[49] V.A. Buryachenko, Applied Mechanics Reviews 54 (2001), p. 1.
[50] L. Brassart, *Homogenization of elasto-(visco)plastic composites: history-dependent incremental and variational approaches*, Ph.D. thesis, The Universit catholique de Louvain, Louvain-la-Neuve (Belgium)., 2011.
[51] I. Doghri and C. Friebel, Mech. of Mater. 37 (2005), pp. 45 – 68.
[52] S. Jansson, Int. J. Solids Struct. 29 (1992), pp. 2181 – 2200.

[53] L. Wu, F. Sket, J.M. Molina-Aldareguia, A. Makradi, L. Adam, I. Doghri, and L. Noels, Composite Structures 126 (2015), pp. 246–264.

Appendix A. Closed-form expression of the derivatives

A.1. *Derivatives of the incremental-secant operator*

In the following $\hat{\mathbb{C}}^{\mathrm{S}}_{i\ n+1}$ will be used to either design $\hat{\mathbb{C}}^{\mathrm{Sr}}_{i\ n+1}$ or $\hat{\mathbb{C}}^{\mathrm{S0}}_{i\ n+1}$ depending on the considered method.

The derivatives of $\hat{\mathbb{C}}^{\mathrm{S}}_{i\ n+1}$ with respect to $\bar{\boldsymbol{\varepsilon}}^{\mathrm{r}}_i$ and $\bar{\boldsymbol{\varepsilon}}^{\mathrm{r}}$ are obtained from (58-61) as follows:

$$\begin{aligned}\frac{\partial\ \hat{\mathbb{C}}^{\mathrm{S}}_{i\ n+1}}{\partial \bar{\boldsymbol{\varepsilon}}^{\mathrm{r}}_i} &= \frac{\partial}{\partial \bar{\boldsymbol{\varepsilon}}^{\mathrm{r}}_i}\left(\mathbb{C}^{\mathrm{el}}_i - 3\mu^{\mathrm{el}}_i\ \Delta\bar{p}_{i\,n+1}\,\frac{\mathbb{I}^{\mathrm{dev}} : \mathbb{C}^{\mathrm{el}}_i}{\left(\Delta\hat{\bar{\sigma}}^{\mathrm{tr}}_{0\mathrm{eq}}\right)}\right)\\ &= -\mathbb{I}^{\mathrm{dev}} \otimes \frac{\partial}{\partial \bar{\boldsymbol{\varepsilon}}^{\mathrm{r}}_i}\left(\frac{2\mu^{\mathrm{el}}_i\ \Delta\bar{p}_{i\,n+1}}{\Delta\hat{\bar{\varepsilon}}^{\mathrm{r}\ \mathrm{eq}}_{i\ n+1}}\right)\\ &= -\frac{2\mu^{\mathrm{el}}_i}{\Delta\hat{\bar{\varepsilon}}^{\mathrm{r}\ \mathrm{eq}}_{i\ n+1}}\mathbb{I}^{\mathrm{dev}} \otimes \frac{\partial\ \Delta\bar{p}_{i\,n+1}}{\partial \bar{\boldsymbol{\varepsilon}}^{\mathrm{r}}_i}\,,\end{aligned} \tag{A1}$$

as $\hat{\bar{\varepsilon}}^{\mathrm{r}\ \mathrm{eq}}_{i\ n+1}$ is being computed from Eqs. (26-27) and does not depend on the strain increment $\bar{\boldsymbol{\varepsilon}}^{\mathrm{r}}_i$.

Using Eqs. (26-27) one has

$$\begin{aligned}\Delta\hat{\bar{\varepsilon}}^{\mathrm{r}\ \mathrm{eq}}_{i\ n+1} &= \sqrt{\frac{2}{3v_i}\mathbb{I}^{\mathrm{dev}} :: \left(\Delta\bar{\boldsymbol{\varepsilon}}^{\mathrm{r}}_{n+1} : \frac{\partial\bar{\mathbb{C}}^{\mathrm{el}}}{\partial\mathbb{C}^{\mathrm{el}}_i} : \Delta\bar{\boldsymbol{\varepsilon}}^{\mathrm{r}}_{n+1}\right)}\\ &= \sqrt{\frac{2}{3v_i}\Delta\bar{\boldsymbol{\varepsilon}}^{\mathrm{r}}_{n+1} : \frac{\partial\bar{\mathbb{C}}^{\mathrm{el}}}{\partial 2\mu^{\mathrm{el}}_i} : \Delta\bar{\boldsymbol{\varepsilon}}^{\mathrm{r}}_{n+1}}\,,\end{aligned} \tag{A2}$$

yielding

$$\frac{\partial\ \Delta\hat{\bar{\varepsilon}}^{\mathrm{r}\ \mathrm{eq}}_{i\ n+1}}{\partial \bar{\boldsymbol{\varepsilon}}^{\mathrm{r}}} = \frac{1}{3v_i\ \Delta\hat{\bar{\varepsilon}}^{\mathrm{r}\ \mathrm{eq}}_{i\ n+1}}\frac{\partial\bar{\mathbb{C}}^{\mathrm{el}}}{\partial\mu^{\mathrm{el}}_i} : \Delta\bar{\boldsymbol{\varepsilon}}^{\mathrm{r}}_{n+1}\,. \tag{A3}$$

From this relation a straightforward result can be obtained:

$$\frac{\partial\ \Delta\hat{\bar{\sigma}}^{\mathrm{tr}\ \mathrm{eq}}_{i}}{\partial \bar{\boldsymbol{\varepsilon}}^{\mathrm{r}}} = \frac{\mu^{\mathrm{el}}_i}{v_i\ \Delta\hat{\bar{\varepsilon}}^{\mathrm{r}\ \mathrm{eq}}_{i\ n+1}}\frac{\partial\bar{\mathbb{C}}^{\mathrm{el}}}{\partial\mu^{\mathrm{el}}_i} : \Delta\bar{\boldsymbol{\varepsilon}}^{\mathrm{r}}_{n+1}\,. \tag{A4}$$

Using (A3), the missing derivative in Eq. (71) reads

$$\begin{aligned}\frac{\partial\,\hat{\mathbb{C}}^{\mathrm{S}}_{i\;n+1}}{\partial\bar{\boldsymbol{\varepsilon}}^{\mathrm{r}}} &= -2\mu_i^{\mathrm{el}}\mathbb{I}^{\mathrm{dev}}\otimes\frac{\partial}{\partial\bar{\boldsymbol{\varepsilon}}^{\mathrm{r}}}\left(\frac{\Delta\bar{p}_{i\,n+1}}{\hat{\bar{\varepsilon}}^{\mathrm{r}\,\mathrm{eq}}_{i\;n+1}}\right)\\ &= 2\mu_i^{\mathrm{el}}\mathbb{I}^{\mathrm{dev}}\otimes\left(\frac{\Delta\bar{p}_{i\,n+1}}{\left(\Delta\hat{\bar{\varepsilon}}^{\mathrm{r}\,\mathrm{eq}}_{i\;n+1}\right)^2}\frac{\partial\Delta\,\hat{\bar{\varepsilon}}^{\mathrm{r}\,\mathrm{eq}}_{i\;n+1}}{\partial\bar{\boldsymbol{\varepsilon}}^{\mathrm{r}}}-\frac{1}{\Delta\hat{\bar{\varepsilon}}^{\mathrm{r}\,\mathrm{eq}}_{i\;n+1}}\frac{\partial\,\Delta\bar{p}_{i\,n+1}}{\partial\bar{\boldsymbol{\varepsilon}}^{\mathrm{r}}}\right)\\ &= 2\mu_i^{\mathrm{el}}\mathbb{I}^{\mathrm{dev}}\otimes\left(\frac{\Delta\bar{p}_{i\,n+1}}{3v_i\left(\Delta\hat{\bar{\varepsilon}}^{\mathrm{r}\,\mathrm{eq}}_{i\;n+1}\right)^3}\frac{\partial\bar{\mathbb{C}}^{\mathrm{el}}}{\partial\mu_i^{\mathrm{el}}}:\Delta\bar{\boldsymbol{\varepsilon}}^{\mathrm{r}}_{n+1}-\frac{1}{\Delta\hat{\bar{\varepsilon}}^{\mathrm{r}\,\mathrm{eq}}_{i\;n+1}}\frac{\partial\,\Delta\bar{p}_{i\,n+1}}{\partial\bar{\boldsymbol{\varepsilon}}^{\mathrm{r}}}\right).\end{aligned}\tag{A5}$$

A.2. *Derivatives of the equivalent plastic strain increment*

To complete the Eqs. (A1) and (A5), one has to evaluate the derivatives of $\Delta\bar{p}_{i\,n+1}$. To this end, the yielding condition (53) is first rewritten as

$$\begin{aligned}F_{\mathrm{Y}} = &\left(\hat{\bar{\sigma}}^{\mathrm{eq}}_{i\;n}\right)^2-\left(\Delta\hat{\bar{\sigma}}^{\mathrm{unload}\,\mathrm{eq}}_{i\;\;n+1}\right)^2-3\,\bar{\boldsymbol{\sigma}}^{\mathrm{res}}_{i\;\;n}:\mathbb{I}^{\mathrm{dev}}:\Delta\bar{\boldsymbol{\sigma}}^{\mathrm{unload}}_{i\;\;n}+\\ &\left(\Delta\hat{\bar{\sigma}}^{\mathrm{tr}\,\mathrm{eq}}_{i\;\;n+1}-3\mu_i^{\mathrm{el}}\,\Delta\bar{p}_{i\,n+1}\right)^2+3\,\bar{\boldsymbol{\sigma}}^{\mathrm{res}}_{i\;\;n}:\mathbb{I}^{\mathrm{dev}}:\Delta\bar{\boldsymbol{\sigma}}^{\mathrm{tr}}_{i\;\;n+1}\\ &-6\mu_i^{\mathrm{el}}\,\Delta\bar{p}_{i\,n+1}\,\bar{\boldsymbol{\sigma}}^{\mathrm{res}}_{i\;\;n}:\mathbb{I}^{\mathrm{dev}}:\hat{\bar{\boldsymbol{N}}}^{\mathrm{tr}}_{i\;\;n+1}-\left(R\left(\bar{p}_{i\,n+1}\right)+\sigma_{\mathrm{Y}_i}\right)^2=0\,.\end{aligned}\tag{A6}$$

This equation in $\Delta\bar{p}_{i\,n+1}$ is solved using a Newton-Raphson scheme at constant values of $\Delta\bar{\boldsymbol{\varepsilon}}^{\mathrm{r}}_i$ and $\Delta\bar{\boldsymbol{\varepsilon}}^{\mathrm{r}}$, yielding

$$\begin{aligned}\frac{\partial F_{\mathrm{Y}}}{\partial\Delta\bar{p}_i} = &-6\mu_i^{\mathrm{el}}\left(\Delta\hat{\bar{\sigma}}^{\mathrm{tr}\,\mathrm{eq}}_{i\;\;n+1}-3\mu_i^{\mathrm{el}}\,\Delta\bar{p}_{i\,n+1}\right)-6\mu_i^{\mathrm{el}}\,\bar{\boldsymbol{\sigma}}^{\mathrm{res}}_{i\;\;n}:\mathbb{I}^{\mathrm{dev}}:\hat{\bar{\boldsymbol{N}}}^{\mathrm{tr}}_{i\;\;n+1}-\\ &2\left(R\left(\bar{p}_{i\,n+1}\right)+\sigma_{\mathrm{Y}_i}\right)\frac{\partial R(\bar{p}_{i\,n+1})}{\partial\bar{p}_i}\,,\end{aligned}\tag{A7}$$

In case the relation (68) is used instead of (53), the second term of the right-hand-side vanishes.

To obtain the derivatives of $\Delta\bar{p}_{i\,n+1}$ with respect to $\Delta\bar{\boldsymbol{\varepsilon}}^{\mathrm{r}}_i$ and $\Delta\bar{\boldsymbol{\varepsilon}}^{\mathrm{r}}$, we assume perturbations of F_Y with these last two fields, which leads to

$$\delta F_{\mathrm{Y}}=\frac{\partial F_{\mathrm{Y}}}{\partial\Delta\bar{\boldsymbol{\varepsilon}}^{\mathrm{r}}_i}:\delta\Delta\bar{\boldsymbol{\varepsilon}}^{\mathrm{r}}_i+\frac{\partial F_{\mathrm{Y}}}{\partial\Delta\bar{p}_i}\delta\Delta\bar{p}_i=0\,,\tag{A8}$$

$$\delta F_{\mathrm{Y}}=\frac{\partial F_{\mathrm{Y}}}{\partial\Delta\bar{\boldsymbol{\varepsilon}}^{\mathrm{r}}}:\delta\Delta\bar{\boldsymbol{\varepsilon}}^{\mathrm{r}}+\frac{\partial F_{\mathrm{Y}}}{\partial\Delta\bar{p}_i}\delta\Delta p_i=0\,,\tag{A9}$$

or again

$$\frac{\partial\Delta\bar{p}_i}{\partial\Delta\bar{\boldsymbol{\varepsilon}}_i{}^{\mathrm{r}}}=-\left(\frac{\partial F_{\mathrm{Y}}}{\partial\Delta\bar{p}_i}\right)^{-1}\frac{\partial F_{\mathrm{Y}}}{\partial\Delta\bar{\boldsymbol{\varepsilon}}_i{}^{\mathrm{r}}}\,,\tag{A10}$$

$$\frac{\partial\Delta p_i}{\partial\Delta\bar{\boldsymbol{\varepsilon}}^{\mathrm{r}}}=-\left(\frac{\partial F_{\mathrm{Y}}}{\partial\Delta\bar{p}_i}\right)^{-1}\frac{\partial F_{\mathrm{Y}}}{\partial\Delta\bar{\boldsymbol{\varepsilon}}^{\mathrm{r}}}\,,\tag{A11}$$

where $\frac{\partial F_{\rm Y}}{\partial \Delta\bar{p}_i}$ is obtained from (A7), and where, using (44) and (A4),

$$\begin{aligned}\frac{\partial F_{\rm Y}}{\partial \Delta\bar{\boldsymbol{\varepsilon}}_i^{\rm r}} &= 3\left(1-\frac{3\mu_i^{\rm el}\,\Delta\bar{p}_{i\,n+1}}{\Delta\hat{\bar{\sigma}}_{i\;n+1}^{\rm tr\;eq}}\right)\bar{\boldsymbol{\sigma}}_{i\;n}^{\rm res} : \mathbb{I}^{\rm dev} : \frac{\partial\,\Delta\bar{\boldsymbol{\sigma}}_{i\;n+1}^{\rm tr}}{\partial\Delta\bar{\boldsymbol{\varepsilon}}_i^{\rm r}} \\ &= 6\mu_i^{\rm el}\left(1-\frac{3\mu_i^{\rm el}\,\Delta\bar{p}_{i\,n+1}}{\Delta\hat{\bar{\sigma}}_{i\;n+1}^{\rm tr\;eq}}\right)\mathbb{I}^{\rm dev} : \bar{\boldsymbol{\sigma}}_{i\;n}^{\rm res}\,, \end{aligned} \tag{A12}$$

$$\begin{aligned}\frac{\partial F_{\rm Y}}{\partial \Delta\bar{\boldsymbol{\varepsilon}}^{\rm r}} &= 2\left(\Delta\hat{\bar{\sigma}}_{i\;n+1}^{\rm tr\;eq}-3\mu_i^{\rm el}\,\Delta\bar{p}_{i\,n+1}\right)\frac{\partial\,\Delta\hat{\bar{\sigma}}_{i\;n+1}^{\rm tr\;eq}}{\partial\bar{\boldsymbol{\varepsilon}}^{\rm r}} + \\ &\quad \frac{9\mu_i^{\rm el}\,\Delta\bar{p}_{i\,n+1}}{\left(\Delta\hat{\bar{\sigma}}_{i\;n+1}^{\rm tr\;eq}\right)^2}\,\bar{\boldsymbol{\sigma}}_{i\;n}^{\rm res} : \mathbb{I}^{\rm dev} : \Delta\bar{\boldsymbol{\sigma}}_{i\;n+1}^{\rm tr}\,\frac{\partial\,\Delta\hat{\bar{\sigma}}_{i\;n+1}^{\rm tr\;eq}}{\partial\bar{\boldsymbol{\varepsilon}}^{\rm r}} \\ &= \left[2\left(\Delta\hat{\bar{\sigma}}_{i\;n+1}^{\rm tr\;eq}-3\mu_i^{\rm el}\,\Delta\bar{p}_{i\,n+1}\right)+\right. \\ &\quad \left.\frac{9\mu_i^{\rm el}\,\Delta\bar{p}_{i\,n+1}}{\left(\Delta\hat{\bar{\sigma}}_{i\;n+1}^{\rm tr\;eq}\right)^2}\,\bar{\boldsymbol{\sigma}}_{i\;n}^{\rm res} : \mathbb{I}^{\rm dev} : \Delta\bar{\boldsymbol{\sigma}}_{i\;n+1}^{\rm tr}\right]\frac{\mu_i^{\rm el}}{v_i\;\Delta\hat{\bar{\varepsilon}}_{i\;n+1}^{\rm r\;eq}}\frac{\partial\bar{\mathbb{C}}^{\rm el}}{\partial\mu_i^{\rm el}} : \Delta\bar{\boldsymbol{\varepsilon}}_{n+1}^{\rm r}\,. \end{aligned} \tag{A13}$$

In case the relation (68) is used instead of (53), the term (A12) and the second term of the right-hand-side of (A13) both vanish.

A.3. *Derivatives of the Eshelby tensor*

In the following the bulk and shear moduli of the LCC phase i, $\hat{\kappa}_{i\,n+1}$ and $\hat{\mu}_{i\,n+1}$, either hold for $\hat{\kappa}_{i\,n+1}^{\rm r}$ and $\hat{\mu}_{i\,n+1}^{\rm r}$ or for $\hat{\kappa}_{i\,n+1}^{0}$ and $\hat{\mu}_{i\,n+1}^{0}$.

The Eshelby tensor depends on the shape of the inclusions and on the Poisson ratio of the matrix material. Thus the derivative of Eshelby tensor can be written as

$$\frac{\partial\mathbb{S}}{\partial\Delta\bar{\boldsymbol{\varepsilon}}_0^{\rm r}} = \frac{\partial\mathbb{S}}{\partial\nu}\otimes\left(\frac{\partial\nu}{\partial\kappa}\frac{\partial\hat{\kappa}_0}{\partial\Delta\bar{\boldsymbol{\varepsilon}}_0^{\rm r}}+\frac{\partial\nu}{\partial\mu}\frac{\partial\hat{\mu}_0}{\partial\Delta\bar{\boldsymbol{\varepsilon}}_0^{\rm r}}\right)\,, \tag{A14}$$

with from (59)

$$\frac{\partial\hat{\kappa}_0}{\partial\Delta\bar{\boldsymbol{\varepsilon}}_0^{\rm r}} = 0\,, \tag{A15}$$

and therefore

$$\frac{\partial\mathbb{S}}{\partial\Delta\bar{\boldsymbol{\varepsilon}}_0^{\rm r}} = \frac{\partial\mathbb{S}}{\partial\nu}\otimes\frac{\partial\nu}{\partial\mu}\frac{\partial\hat{\mu}_0}{\partial\Delta\bar{\boldsymbol{\varepsilon}}_0^{\rm r}}\,. \tag{A16}$$

Similarly, the derivatives with the composite strain increment reads

$$\frac{\partial\mathbb{S}}{\partial\Delta\bar{\boldsymbol{\varepsilon}}^{\rm r}} = \frac{\partial\mathbb{S}}{\partial\nu}\otimes\frac{\partial\nu}{\partial\mu}\frac{\partial\hat{\mu}_0}{\partial\Delta\bar{\boldsymbol{\varepsilon}}^{\rm r}}\,. \tag{A17}$$

The remaining two terms $\frac{\partial\hat{\mu}_0}{\partial\Delta\bar{\boldsymbol{\varepsilon}}_0^{\rm r}}$ and $\frac{\partial\hat{\mu}_0}{\partial\Delta\bar{\boldsymbol{\varepsilon}}^{\rm r}}$ are obtained from Eq. (61) using Eqs.

(A3), (A10) and (A11).

A.4. *Derivative of the MFH residual*

In the following $\hat{\mathbb{C}}^{\mathrm{S}}_{i\ n+1}$ will be used to either design $\hat{\mathbb{C}}^{\mathrm{Sr}}_{i\ n+1}$ or $\hat{\mathbb{C}}^{\mathrm{S0}}_{i\ n+1}$ depending on the considered method. Similarly,

Starting from (89)

$$\begin{aligned}\boldsymbol{F} = \hat{\mathbb{C}}^{\mathrm{S}}_{0\,n+1} : \left[\Delta\bar{\boldsymbol{\varepsilon}}^{\mathrm{r}}_{\mathrm{I}\,n+1} - \frac{1}{v_0}\mathbb{S}^{-1} : (\Delta\bar{\boldsymbol{\varepsilon}}^{\mathrm{r}}_{\mathrm{I}\,n+1} - \Delta\bar{\boldsymbol{\varepsilon}}^{\mathrm{r}}_{n+1})\right] - \\ \hat{\mathbb{C}}^{\mathrm{S}}_{\mathrm{I}\,n+1} : \Delta\bar{\boldsymbol{\varepsilon}}^{\mathrm{r}}_{\mathrm{I}\,n+1}\ ,\end{aligned} \tag{A18}$$

we have

$$\begin{aligned}\frac{\partial \boldsymbol{F}}{\partial \bar{\boldsymbol{\varepsilon}}} = \left[\Delta\bar{\boldsymbol{\varepsilon}}^{\mathrm{r}}_{\mathrm{I}\,n+1} - \frac{1}{v_0}\mathbb{S}^{-1} : (\Delta\bar{\boldsymbol{\varepsilon}}^{\mathrm{r}}_{\mathrm{I}\,n+1} - \Delta\bar{\boldsymbol{\varepsilon}}^{\mathrm{r}}_{n+1})\right] : \frac{\partial\, \hat{\mathbb{C}}^{\mathrm{S}}_{0\,n+1}}{\partial \bar{\boldsymbol{\varepsilon}}} + \\ \frac{1}{v_0}\,\hat{\mathbb{C}}^{\mathrm{S}}_{0\,n+1} \otimes \left(\Delta\bar{\boldsymbol{\varepsilon}}^{\mathrm{r}}_{\mathrm{I}\,n+1} - \Delta\bar{\boldsymbol{\varepsilon}}^{\mathrm{r}}_{n+1}\right) :: \left(\mathbb{S}^{-1} \otimes \mathbb{S}^{-1}\right) :: \frac{\partial \mathbb{S}}{\partial \bar{\boldsymbol{\varepsilon}}} + \\ \frac{1}{v_0}\,\hat{\mathbb{C}}^{\mathrm{S}}_{0\,n+1} : \mathbb{S}^{-1} - \Delta\bar{\boldsymbol{\varepsilon}}^{\mathrm{r}}_{\mathrm{I}\,n+1} : \frac{\partial\, \hat{\mathbb{C}}^{\mathrm{S}}_{\mathrm{I}\,n+1}}{\partial \bar{\boldsymbol{\varepsilon}}}\,.\end{aligned} \tag{A19}$$

where $\frac{\partial\, \hat{\mathbb{C}}^{\mathrm{S}}_{i\ n+1}}{\partial \bar{\boldsymbol{\varepsilon}}}$ result from (A5), and where $\frac{\partial \mathbb{S}}{\partial \bar{\boldsymbol{\varepsilon}}}$ results from (A17).